AD-A130 202 THE AIR WEATHER SERVICE PRIMITIVE EQUATION MODELS PART 1/1
1 THE 6-LAYER AWSP..(U) AIR FORCE GLOBAL WEATHER
CENTRAL OFFUTT AFB NE T C TARBELL ET AL. MAY 82
UNCLASSIFIED AFGWC/TN-82-001 SBI-AD-E850 382 F/G 4/2 NL

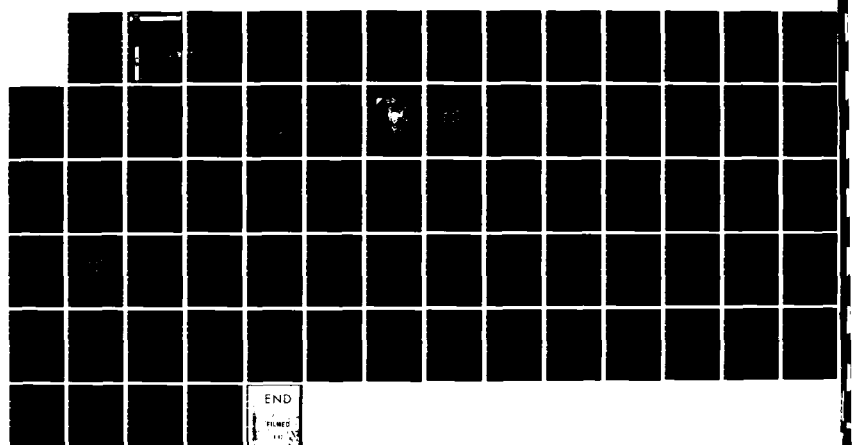

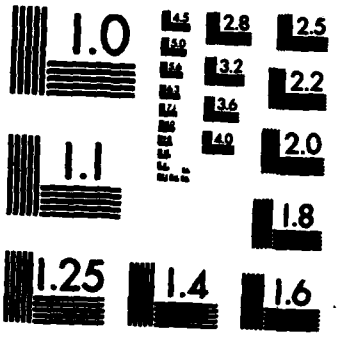

AFGWC/TN 82/001

THE AIR WEATHER SERVICE PRIMITIVE EQUATION MODELS

PART I: THE SIX-LAYER AWSPE MODEL

By

Maj Terry C. Tarbell

Capt Fred P. Lewis

11 1 APR 1983
1 APR 1983

PART II: THE SEVEN-LAYER AWSPE MODEL

By

Capt Fred P. Lewis

Maj Terry C. Tarbell

1Lt Larry G. Renninger

1Lt Allen M. Weiner

MAY 1982

UNITED STATES AIR FORCE
AIR WEATHER SERVICE (MAC)
AIR FORCE GLOBAL WEATHER CENTRAL
OFFUTT AFB NE 68113

REVIEW AND APPROVAL STATEMENT

This publication approved for public release. There is no objection to unlimited distribution of this document to the public at large, or by the Defense Technical Information Center (DTIC) or to the National Technical Information Service (NTIS).

This technical publication has been reviewed and is approved for publication.

Charles W Cook

CHARLES W. COOK, GM-13, DAFC
Reviewing Official

FOR THE COMMANDER

Kenneth E German

KENNETH E. GERMAN, Colonel, USAF
Chief, Technical Services Division

ERRATA

1. Page 3, ASWPE MODEL CHARACTERISTICS should read: "THE 6-LAYER AWSPE MODEL CHARACTERISTICS."

2. Page 12, equation (3.16) where $(\sigma_\beta)_6=0$, $\Delta\sigma=1$, should read: "$(\dot{\sigma}_\beta)_6=0$; $\Delta\sigma=1$"

3. Page 14, equation (3.30) $\Delta\cdot(K\Delta u)$ should read: "$\nabla\cdot(K\nabla u)$."

4. Page 15, equation (3.31) $\Delta\cdot(K\Delta v)$ should read: "$\nabla\cdot(K\nabla v)$."

5. Page 15, equation (3.33) should read: "$\psi^{(n)*} = \psi^n + \alpha(\psi^{(n-1)*} - 2\psi^n + \psi^{n+1})$."

6. Page 34, equation (12.15) should read: "$\overline{\qquad\qquad\qquad\qquad\qquad\qquad\qquad\qquad}^{x_h y_h}_{\sigma}$"

$$\frac{\partial\theta}{\partial t} = -\overline{m^2}^{xy}\left(\overline{u}^{xy}\overline{\theta}^{y}_{y_h} + \overline{v}^{xy}\overline{\theta}^{x}_{x_h}\right) - \left(\dot{\sigma}\overline{\theta}^{xy}_{\sigma}\right)$$

7. Page 34, equation (12.17) should read:

$$\overline{p}^{t}_{\sigma_t} = 0 = -\overline{m^2}^{xy}\left(\overline{u}^{xy}\overline{p}^{y}_{\sigma_x} + \overline{v}^{xy}\overline{p}^{x}_{\sigma_y} + \overline{p}^{xy}_{\sigma}\left(\overline{u}^{y}_{x} + \overline{v}^{x}_{y}\right)\right) - \overline{p}^{xy}_{\sigma}\dot{\sigma}_{\sigma}$$

8. Page 34, equation (12.18) should read: "$(\dot{\sigma}_{\beta_\sigma})_6 = \dfrac{(\dot{\sigma}_\beta)_7 - (\dot{\sigma}_\beta)_6}{\Delta\sigma} = -(\dot{\sigma}_\beta)_6$"

9. Page 35, equation (12.19) where $(\sigma_\beta)_7=0$; $\Delta\sigma=1$ should read: "$(\dot{\sigma}_\beta)_7 = 0$; $\Delta\sigma = 1$"

10. Page 36, equation (12.24), bottom equation should read:

$$"(\dot{\sigma}_T)_5 + (\dot{\sigma}_T)_3 = (2\,\dot{\sigma}_T)_4 = \Delta\sigma^2 D_4"$$

11. Page 41, equation (12.41) should read:

$$"\phi_1 = \hat{\phi}_1 + C_p\left\{\sum_{k=1}^{k-1}\hat{\sigma}_{k+1}\left\{(\theta_k - \theta_{k+1})\left[\tfrac{1}{2}(\pi_k + \pi_{k+1}) - \hat{\pi}_{k+1}\right]\right\} + \theta_1(\hat{\pi}_1 - \pi_1)\right\}$$

12. Page 42, equation (12.43) should read:

$$" \int_{z_\beta}^{z_T} C_p\,\delta T\,dz = \frac{C_p}{g}\int_{p_T}^{p_\beta}\delta T\,dp = 0$$

UNCLASSIFIED

SECURITY CLASSIFICATION OF THIS PAGE (When Data Entered)

REPORT DOCUMENTATION PAGE		READ INSTRUCTIONS BEFORE COMPLETING FORM
1. REPORT NUMBER AFGWC/TN-82-001	2. GOVT ACCESSION NO. AD-A130 202	3. RECIPIENT'S CATALOG NUMBER
4. TITLE (and Subtitle) The Air Weather Service Primitive Equation Models. Part I: The Six-Layer AWSPE Model. Part II: The Seven-Layer AWSPE Model.		5. TYPE OF REPORT & PERIOD COVERED 6. PERFORMING ORG. REPORT NUMBER
7. AUTHOR(s) Terry C. Tarbell Fred P. Lewis		8. CONTRACT OR GRANT NUMBER(s)
9. PERFORMING ORGANIZATION NAME AND ADDRESS HQ Air Force Global Weather Central (MAC) Offutt AFB, Nebreaska 68113		10. PROGRAM ELEMENT, PROJECT, TASK AREA & WORK UNIT NUMBERS
11. CONTROLLING OFFICE NAME AND ADDRESS HQ Air Force Global Weather Central (MAC) Offutt AFB, Nebraska 68113		12. REPORT DATE May, 1982 13. NUMBER OF PAGES 60 + vi
14. MONITORING AGENCY NAME & ADDRESS(if different from Controlling Office) HQ Air Force Global Weather Central (MAC) Offutt AFB, Nebraska 68113		15. SECURITY CLASS. (of this report) Unclassified 15a. DECLASSIFICATION/DOWNGRADING SCHEDULE

16. DISTRIBUTION STATEMENT (of this Report)

Approved for public release; distribution unlimited.

17. DISTRIBUTION STATEMENT (of the abstract entered in Block 20, if different from Report)

N/A

18. SUPPLEMENTARY NOTES

19. KEY WORDS (Continue on reverse side if necessary and identify by block number)

Numerical Weather Prediction
Air Force Global Weather Central
National Meteorological Center
Primitive equation models
Shuman-Hovermale PE model
* models

20. ABSTRACT (Continue on reverse side if necessary and identify by block number)

This Technical Note describes the Air Weather Service Primitive-Equation (AWSPE) models in use at the Air Force Global Weather Central (AFGWC). There are 6-layer and 7-layer AWSPE versions. We present a brief history of the models at AFGWC as well as their forerunners at the National Meteorological Center. We then present the technical details of both models. Parts I and II describe the 6-layer and 7-layer versions, respectively.

DD FORM 1 JAN 73 1473 EDITION OF 1 NOV 65 IS OBSOLETE

UNCLASSIFIED

SECURITY CLASSIFICATION OF THIS PAGE (When Data Entered)

PREFACE

The purpose of this Technical Note (TN) is to describe the Air Weather Service Primitive Equation (AWSPE) models, both the 6-layer (6L) and 7-layer (7L) versions. We will present a brief history of the models at the Air Force Global Weather Central (AFGWC) as well as their forerunners at the National Meteorological Center (NMC). We will then present the technical details of the AWSPE models. In Part II we will describe the new 7L AWSPE model.

This publication could not have been completed without the assistance of many people:

- Mr. Ken Campana, NMC Development Division, for very valuable discussions about his work with the NMC 7L PE model.

- Lieutenant Colonel James Kerlin, formerly AFGWC Liaison Officer to NMC, for providing the NMC 7L PE model software and many useful NMC Office Notes.

- Major Doug Moore, formerly AFGWC/TSIN, for his help in developing the 7L AWSPE model.

- Major John Warburton, AFGWC Liaison Officer to NMC, for providing much useful information on the NMC 7L PE.

- Captain (Dr) James Hoke, formerly AFGWC/TSIN, for his help in developing the 7L AWSPE model.

- The following reviewers, for their valuable comments and suggestions:

Colonel Kenneth E. German (TS)
Mr. Charles W. Cook (TSA)
Major Randolph W. Ashby (TSI)
Major John Burgeson (NSM)
Captain Kenneth E. Mitchell (TSIT)
Lieutenant Jason P. Tuell (TSIN)

- The following AFGWC personnel for their clerical help and administrative support:

Chief Master Sergeant Horace Maxwell (TSA)
Sergeant Roger Jones (TSA)
AlC Sam Gomez
Miss Mary Ann Kosmicki (DAW)
Mrs. Melissa Hockman (DAW)

Major Terry C. Tarbell
Captain Fred P. Lewis
First Lieutenant Larry G. Renninger
First Lieutenant Allan M. Weiner

1 May 1982

TABLE OF CONTENTS

LIST OF TABLES

LIST OF FIGURES

LIST OF ABBREVIATIONS

AFGWC	Air Force Global Weather Central
AWN	Automated Weather Network
AWSPE	Air Weather Service Primitive Equation Model
BDI	Bank Description Index
CDC	Control Data Corporation
GMT	Greenwich Mean Time
HIANAL	AFGWC High-Level Analysis Model
HUPANL	AFGWC Hough Spectral Analysis Model
I/O	Input/Output
NMC	National Meteorological Center
NWP	Numerical Weather Prediction
PBL	Planetary Boundary Layer
SIXLVL	AFGWC Six-Level Quasi-Geostrophic Forecast Model
TN	Technical Note
TSIN	Numerical Forecasting Section
1MPROG	AFGWC 1000-mb Prognosis Model
PE	Primitive Equation
6L	Six-Layer
6L PE	Six-Layer Primitive Equation Model
7L	Seven-Layer
7L PE	Seven-Layer Primitive Equation Model

PART I: The 6-Layer AWSPE Model

Major Terry C. Tarbell
Captain Fred P. Lewis

1. INTRODUCTION

The Air Weather Service Primitive-Equation (AWSPE) model, also referred to as the 6-Layer (6L) AWSPE, is a dry version (that is, no moisture variable is forecast) of the Shuman-Hovermale model (Shuman and Hovermale, 1968). Before discussing the history of the 6L AWSPE, it is appropriate to present a brief history of the Shuman-Hovermale model.

1.1 The Shuman-Hovermale Model at NMC.

On 6 June 1966, the Shuman-Hovermale six-layer primitive-equation (6L PE) model became operational at NMC (this entire subsection was adapted from Shuman and Hovermale, 1968). The 6L PE was the first primitive-equation (PE) model used operationally anywhere.

The 6L PE model replaced the Cressman (1963) three-level filtered equation model. The Cressman model and its predecessors at NMC were all based on Rossby's (1939) idea that the principle mechanism in the short-term prediction of large-scale atmospheric motions is the conservation of the vertical component of absolute vorticity. The application of Rossby's idea leads to the use of differentiated forms of the equations of motion rather than the "primitive" equations themselves. Charney (1962) neglected the time-rate-of-change-of-divergence term in the divergence equation. The resulting equations are called "balance equations" and these equations "filter" or eliminate the fastest moving waves (inertia-gravity waves) permitted by the primitive equations. Thus, the only motions permitted by the filtered equations are the slowly moving meteorological waves of interest.

By 1959, NMC scientists realized that further advances in numerical weather prediction (NWP) would be severely limited unless the primitive equations themselves were used. This led to the development of the 6L PE model between 1959 and 1966. Many obstacles, such as computational instability, had to be overcome in the development of the model. After the 6L PE was developed, it did not meet operational timelines because it required many more calculations than the Cressman model. However, two events occurred that made operational use of the model feasible:

a. The development of a new generation of computers and the installation of one of them (a CDC-6600) at NMC.

b. The Automated Weather Network (AWN) that collected data significantly faster than before, thereby permitting an earlier 6L PE start time. The operational implementation of the Shuman-Hovermale model will always be remembered as a major achievement in the field of numerical weather prediction.

1.2 Performance of the Shuman-Hovermale Model.

Shuman and Hovermale (1968) presented the S-1 scores (Teweles and Wobus, 1954) for the months between June 1966 and August 1967 for the barotropic model 36-h 500-mb forecasts and for the 6L PE 36-h 500-mb forecasts. The 6L PE model set the record low S-1 score for any month four times and set records for seven months of the year. The 6L PE S-1 scores beat the barotropic model S-1 scores by an average of 6 points for the 15-month verification period. Since an improvement in S1 score of 4 points is considered good, an improvement of 6 points is indeed impressive.

Many other statistics also led to the conclusion that the 6L PE was far superior to the Cressman model. Thus, the use of primitive-equation models to forecast the atmosphere was firmly established.

1.3 A 6-Layer Primitive-Equation Model at AFGWC.

The 6-Layer AWSPE (6L AWSPE), a version of the Shuman-Hovermale model, was implemented at AFGWC on 4 May 1975. The 6L AWSPE was the first primitive-equation model to be used at AFGWC. It currently runs four times daily in the Northern Hemisphere producing 72-h forecasts for the 00 and 12 GMT data times and 36-h forecasts for the 06 and 18 GMT data times. Tarbell and Hoke (1979) presented a description of how the 6L AWSPE fits in the operational production system at AFGWC.

The previous operational forecast model at AFGWC was SIXLVL, the Six-Level Quasi-geostrophic Forecast Model, described by Palucci (1970). Unlike the 6L AWSPE, SIXLVL is a filtered model. Flattery (1975) reported that the formulation of SIXLVL is based on a number of assumptions and approximations including:

a. The horizontal wind is assumed to be nondivergent.

b. The static stability is a function of pressure only.

c. An artificial term is included to stabilize the long waves.

d. Surface friction is included only in the form of a modified vertical velocity.

e. The Coriolis parameter, f, is assumed to be constant for certain equation terms.

f. Some smaller-magnitude terms have been omitted from the model equations.

The 6L AWSPE model does not use any of these assumptions. Thus, after implementing the 6L AWSPE model, AFGWC realized improved forecasts similar to the improved forecasts that occurred at NMC after implementation of the 6L PE. Major differences between 6L AWSPE and the SIXLVL combination can be expected in vertical velocity and vorticity. In the SIXLVL model, vertical velocity fields are dependent only on the stream function. In the 6L AWSPE model, the vertical velocity field is derived directly from the total rate of

change with respect to time in the pressure field and therefore can be quite different in both detail and magnitude.

In the SIXLVL model, the winds are diagnosed and remain nearly geostrophic. In the 6L AWSPE model, the wind components themselves are forecast and significant ageostrophic components result. Thus, the 6L AWSPE vorticity centers can be displaced from the positions that would be expected from the height-contour pattern.

Since SIXLVL's lowest forecast level is 850 mb, another forecast model is used to provide surface forecasts. Originally developed by Reed (1963), 1MPROG produces the 1000-mb forecast by advecting the 1000-500 mb thickness with a portion of the 500-mb wind field. In the 6L AWSPE model, surface forecasts are obtained through the dynamic evolution of the three-dimensional model atmosphere using a terrain-following coordinate system.

The remainder of Part I of this Tech Note gives a technical description of the 6L AWSPE model. Section 2 contains a description of the vertical and horizontal model domains and the set of primitive equations used. In Section 3, we present the model finite-difference equations and other physical parameterizations. In Section 4, the sequence of calculations used to compute the forecast are detailed. Section 5 contains the procedure used to initialize the 6L AWSPE. In Section 6, we present the procedure used to calculate the forecast fields on mandatory pressure surfaces. Section 7 contains a comparison of the 6L AWSPE with the original Shuman-Hovermale model. Section 8 describes the subroutines in the 6L AWSPE and contains a basic subroutine flow diagram for the model. This section is mainly for use by AFGWC/TSIN programmers and may be skipped by other readers. Section 9 is a summary of Part I.

2. ASWPE MODEL CHARACTERISTICS

2.1 The Primitive Equations.

The hydrostatic meteorological equations for a model with a vertical sigma coordinate and horizontal Cartesian coordinates on a conformal polar stereographic projection of the earth are given by Shuman and Hovermale (1968). They are:

$$\frac{\partial u}{\partial t} + \dot{\sigma}\frac{\partial u}{\partial \sigma} - v\left(f - v\frac{\partial m}{\partial x} + u\frac{\partial m}{\partial y}\right) + m\left(u\frac{\partial u}{\partial x} + v\frac{\partial u}{\partial y} + \frac{\partial gz}{\partial x} + c_p\theta\frac{\partial \pi}{\partial x}\right) + F_x = 0, \tag{2.1}$$

$$\frac{\partial v}{\partial t} + \dot{\sigma}\frac{\partial v}{\partial \sigma} + u\left(f - v\frac{\partial m}{\partial x} + u\frac{\partial m}{\partial y}\right) + m\left(u\frac{\partial v}{\partial x} + v\frac{\partial v}{\partial y} + \frac{\partial gz}{\partial y} + c_p\theta\frac{\partial \pi}{\partial y}\right) + F_y = 0, \tag{2.2}$$

$$\frac{\partial gz}{\partial \sigma} + c_p \theta \frac{\partial \pi}{\partial \sigma} = 0, \tag{2.3}$$

$$\frac{\partial \theta}{\partial t} + \dot{\sigma}\frac{\partial \theta}{\partial \sigma} + m\left(u\frac{\partial \theta}{\partial x} + v\frac{\partial \theta}{\partial y}\right) + H = 0, \tag{2.4}$$

$$\frac{\partial}{\partial t}\left(\frac{\partial p}{\partial \sigma}\right) + \frac{\partial}{\partial \sigma}\left(\frac{\partial p}{\partial \sigma}\dot{\sigma}\right) + m\left[\frac{\partial}{\partial x}\left(\frac{\partial p}{\partial \sigma}u\right) + \frac{\partial}{\partial y}\left(\frac{\partial p}{\partial \sigma}v\right)\right] - \frac{\partial p}{\partial \sigma}\left(u\frac{\partial m}{\partial x} + v\frac{\partial m}{\partial y}\right) = 0, \tag{2.5}$$

$$\pi = \left(\frac{p}{p_o}\right)^{R/c_p} \tag{2.6}$$

where σ is defined as:

$$\sigma = \frac{p - p_v}{p_L - p_v} \tag{2.7}$$

These six equations are written in the six dependent variables u, v, σ, θ, π, and p. It is worth noting that x and y are the two horizontal Cartesian coordinates on the projection while u and v are the x and y components of velocity true on the earth. The map factor, m, is the ratio of a distance on the projection to the corresponding distance on the earth. Therefore, we can write

$$u_{proj} = mu \tag{2.8}$$

$$v_{proj} = mv \tag{2.9}$$

where U_{proj} and V_{proj} are the horizontal velocity components on the conformal projection.

The definition of sigma given by (2.7) is a generalization of Phillips (1957) vertical coordinate $\sigma = p/p^*$, where p^* is surface pressure.

2.2 The Vertical Domain.

Fig. 2.1 is a depiction of the vertical structure of the 6L AMSPE model. The model contains four separate sigma domains that contain the seven vertical layers. The lowest sigma domain is a planetary boundary layer with the vertical coordinate defined by

$$\sigma_B = \frac{p - p_5}{p_6^* - p_5} \quad . \tag{2.10}$$

The second sigma domain consists of three layers and constitutes the remainder of the troposphere. The second sigma domain is defined by

$$\sigma_T = \frac{p - p_2^{**}}{p_5 - p_2^{**}} \tag{2.11}$$

where p_2^{**} is the pressure at the tropopause. The tropopause is considered to be a material surface; that is, $\sigma_2 = 0$.

The third sigma domain consists of two layers and constitutes the model stratosphere. The stratospheric domain is defined by

$$S = \frac{p-p_0}{p_2^{**}-p_0} \tag{2.12}$$

where p_0 is the pressure at the top of the model ($\sim$100mb).

The level at the top of the stratosphere (k=0) is also treated as a material surface.

The topmost sigma domain is a layer of constant potential temperature. It is defined by

$$\sigma_\theta = \frac{p}{p_\theta} \quad . \tag{2.13}$$

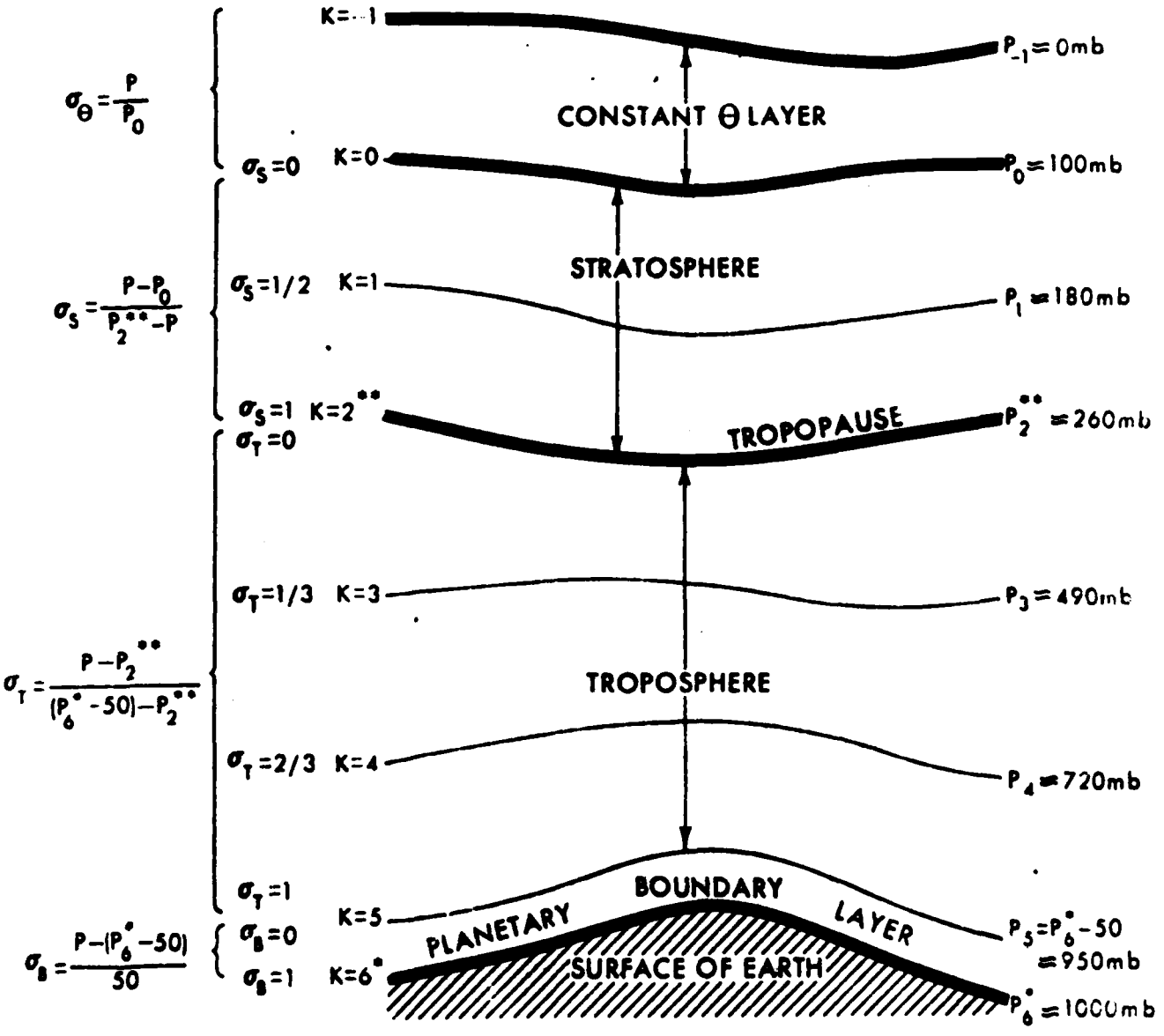

Figure 2.1. Depiction of the vertical structure of the 6L AWSPE model.

This seventh layer is included for its computational rather than its meteorological properties.

2.3 The Horizontal Grid.

The horizontal grid is a regular square mesh on a polar stereographic projection true at 60N. For this projection,

$$m = (1 + \sin 60)/(1 + \sin \phi) \tag{2.14}$$

where Φ is north latitude. Centered at the North Pole, the horizontal grid consists of 53 X 57 (3021) points (see Fig. 2.2). The grid increment is one bedient (381 km) at 60N. The AFGWC Northern Hemisphere octagon grid is a subset of points within the ANSPE horizontal grid (see Hoke et al., 1981). Model forecasts produced outside the octagon are not used. The boundary conditions at the edge of the rectangular grid and the initialization technique employed between the octagon and the rectangular grid combine to produce less reliable forecasts outside the octagon. The lateral boundary conditions and the initialization procedure are discussed in later sections. The purpose of the boundary region is to provide a buffer zone between the walls and the active meteorological areas.

2.4 Prognostic and Diagnostic Variables.

The forecast or history variables are u, v, θ, and p_σ. The diagnosed variables are π, z, $\dot{\sigma}$, and p. In Fig. 2.3, we show that u, v, and θ are defined at the half levels and p, π, $\dot{\sigma}$, and z are defined at the full levels. Actually, $\dot{\sigma}$ is defined at the center point of each square formed by four grid points at which z, π, and p are defined (see Fig. 2.3). The methods used to calculate these variables are presented in sections 3 and 4.

3. FINITE-DIFFERENCE FORMULATION OF THE ANSPE MODEL.

In this section, we will present the model finite-difference equations, the PBL friction parameterization, the method of calculating $\dot{\sigma}$, the lateral boundary conditions, the horizontal smoothing and the time smoothing, the pressure-gradient-averaging methods, and the techniques used to compute omega (ω), which is the vertical motion in pressure coordinates.

3.1 ANSPE Finite-Difference Equations.

Shuman and Hovermale (1968) introduced a convenient short-hand notation for the description of finite-difference formulations which is now used almost universally. Differencing and averaging in the x-direction are written as

$$f_x = \frac{f_{i+\frac{1}{2}} - f_{i-\frac{1}{2}}}{x_{i+\frac{1}{2}} - x_{i-\frac{1}{2}}} \tag{3.1}$$

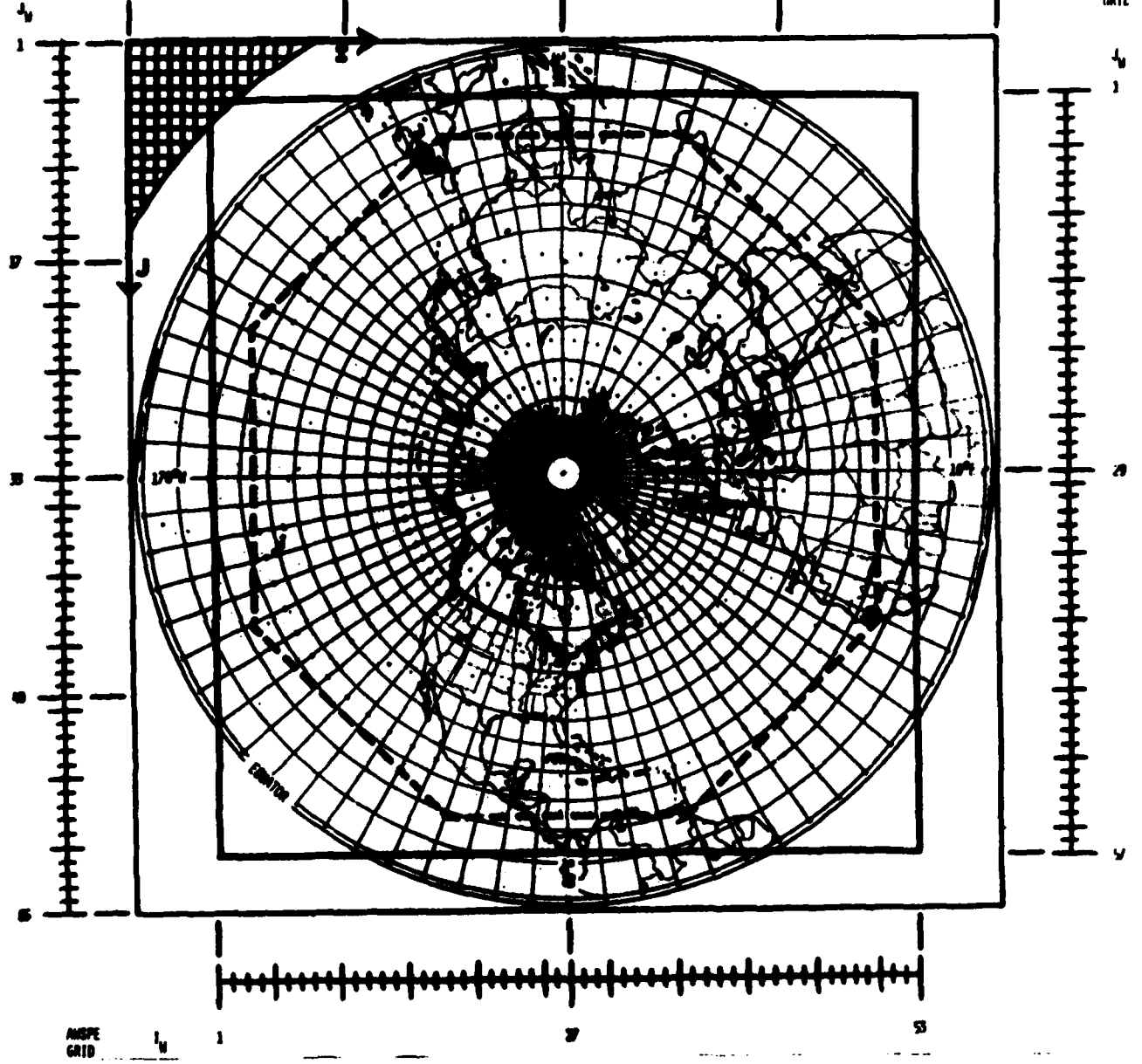

Figure 2.2. The AFGWC northern hemisphere whole-mesh grid for the 6L and 7L AWSPE models is given by the inner solid lines. The domains of the Northern Hemispheric Reference Grids (solid outer border) and the Octagon grids (dashed lines) are also indicated. The indices (I_W, I_W) designate the coordinates for both the Whole-mesh Reference Grid and the AWSPE grid. The whole mesh grid spacing is displayed in the upper-left corner.

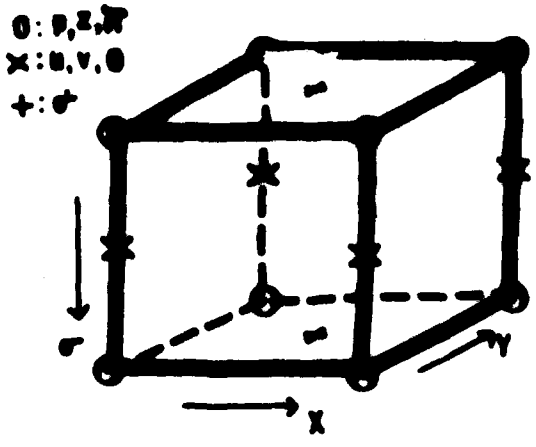

Figure 2.3. Schematic box connecting eight adjacent grid points, taken from Shuman and Hovermale (1968).

$$\bar{f}^{x} = \tfrac{1}{2}(f_{i+\frac{1}{2}} + f_{i-\frac{1}{2}}) \tag{3.2}$$

where i is the serial number of a point in the x direction. The use of more than one superscript or subscript means

$$f_{xx} = (f_x)_x \tag{3.3}$$

$$\bar{f}^{xx} = \overline{(\bar{f}^{x})}^{x} \tag{3.4}$$

Values of f are defined at grid points on the horizontal grid. Therefore, values of f_x and $\bar{f}^{x}$ represent values between grid points. The following combinations of operations are examples of common finite-difference operations:

$$\bar{f}^{x}_{x} = \frac{f_{i+1} - f_{i-1}}{x_{i+1} - x_{i-1}} \tag{3.5}$$

$$f_{xx} = \frac{f_{i+1} - 2f_i + f_{i-1}}{(x_{i+\frac{1}{2}} - x_{i-\frac{1}{2}})} \tag{3.6}$$

Using the Shuman-Hovermale finite-difference notation, the finite-difference representations of (2.1) through (2.5) are written:

$$\bar{u}^{t}_{t} + \overline{[\overline{(\dot{\sigma}\bar{u}^{xy})}^{\sigma}_{\sigma} - \bar{v}^{xy}(\bar{f}^{xy} - \bar{v}^{xy}\bar{m}^{y}_{x} + \bar{u}^{xy}\bar{m}^{x}_{y}) + F_x]}^{xy} + \overline{[\bar{m}^{xy}(\bar{u}^{xy}\bar{u}^{y}_{x} + \bar{v}^{xy}\bar{u}^{x}_{y} + g\bar{z}^{\sigma y} + c_p\bar{\theta}^{xy}\bar{\pi}^{\sigma y}_{x})]}^{xy} = 0, \tag{3.7}$$

$$\bar{v}^{t}_{t} + \overline{[(\dot{\sigma}\bar{v}^{xy}_{\sigma})^{\sigma} + \bar{u}^{xy}(\bar{f}^{xy} - \bar{v}^{xy}\bar{m}^{x}_{y}) + F_{y}]}^{xy}$$

$$+\overline{[\bar{m}^{xy}(\bar{u}^{xy}\bar{v}^{y}_{x} + \bar{v}^{xy}\bar{v}^{y}_{x} + g\bar{z}^{\sigma x}_{y} + c_{p}\bar{\theta}^{xy}\bar{\pi}^{\sigma x}_{y})]}^{xy} = 0, \tag{3.8}$$

$$gz_{\sigma} + c_{p}\theta\pi = 0, \tag{3.9}$$

$$\bar{\theta}^{t}_{t} + \overline{[(\dot{\sigma}\bar{\theta}^{xy}_{\sigma})^{\sigma} + \bar{m}^{xy}(\bar{u}^{xy}\bar{\theta}^{y}_{x} + \bar{v}^{xy}\bar{\theta}^{x}_{y}) + H]}^{xy} = 0, \tag{3.10}$$

$$\bar{p}^{t}_{\sigma t} + \overline{[\bar{p}^{xy}_{\sigma}\dot{\sigma}_{\sigma} + \bar{m}^{xy}(\bar{u}^{xy}\bar{p}^{y}_{\sigma x} + \bar{v}^{xy}\bar{p}^{x}_{\sigma y})]}^{xy}$$

$$+ \overline{\{\bar{p}^{xy}_{\sigma}[\bar{m}^{xy}(\bar{u}^{y}_{x} + \bar{v}^{x}_{y}) - \bar{u}^{xy}\bar{m}^{x}_{y}]\}}^{xy} = 0 . \tag{3.11}$$

The $\widetilde{(\ )}^{t}$ over the pressure-gradient-force terms in (3.7) and (3.8) represents the pressure-averaging technique of Brown and Campana (1978). In this technique, the pressure-gradient force is computed at three time steps (t+1, t, and t-1, where t is the time step) and then averaged as follows:

$$\widetilde{(\ )}^{t} = \alpha[(\ )^{t+1} + (\ )^{t-1}] + (1 - 2\alpha)(\ )^{t} . \tag{3.12}$$

This technique is numerically stable for $\alpha = 0.25$. In practice, $\alpha = 0.245$ for the first six forecast hours and is then set at $\alpha = 0.25$ for the remainder of the forecast. The pressure-gradient-averaging technique allows the time step used by the model to be doubled.

3.2 PBL Friction.

Frictional dissipation is only considered in the model boundary layer. Thus, vertical momentum exchange due to turbulent (subgrid-scale) eddies is parameterized in the model boundary layer. The friction terms F_x and F_y in (3.7) and (3.8) have the following forms:

$$F_x = \frac{g\rho}{\Delta p} C_D [(\bar{u}^{xy})^2 + (\bar{v}^{xy})^2]^{\frac{1}{2}} \bar{u}^{xy} \tag{3.13}$$

$$F_y = \frac{g\rho}{\Delta p} C_D [(\bar{u}^{xy})^2 + (\bar{v}^{xy})^2]^{\frac{1}{2}} \bar{v}^{xy} \tag{3.14}$$

where ρ is the standard sea-level density and $\Delta p = 50$ mb. The drag coefficient, C_D, is modeled after Cressman (1960) and has a large horizontal variation that is positively correlated with terrain height.

3.3 The Calculation of "Sigma Dot".

The method used for computing $\dot{\sigma}$ follows almost directly from the finite difference form of the p_σ tendency equation (3.11) and the fact that $\dot{\sigma} = 0$ at levels $\sigma = 6^*, 2^{**}, 0$, and -1.

First, $p_\sigma = 50$ mb in the boundary layer and is constant in time and space. Thus, if we remove the $\overline{(\,)}^{xy}$ operator, (3.11) may be written as

$$(\dot{\sigma}_{B\sigma})_5 = -[(\bar{m}^{xy}(\bar{u}^y_x + \bar{v}^x_y) - (\bar{u}^{xy}\bar{m}^y_x + \bar{v}^{xy}\bar{m}^x_y)], \tag{3.15}$$

but,

$$(\dot{\sigma}_{B\sigma})_5 = \frac{(\dot{\sigma}_B)_6 - (\dot{\sigma}_B)_5}{\Delta\sigma} = -(\dot{\sigma}_B)_5 \tag{3.16}$$

where

$$(\sigma_B)_6 = 0, \quad \Delta\sigma = 1$$

and

$$(\dot{\sigma}_B)_5 = \bar{m}^{xy}(\bar{u}^y_x + \bar{v}^x_y) - (\bar{u}^{xy}\bar{m}^y_x + \bar{v}^{xy}\bar{m}^x_y) \quad . \tag{3.17}$$

In the troposphere, a different approach must be used, since p_σ varies in time and space. However, p_σ must be linear with respect to σ, therefore $p_{\sigma\sigma} = 0$. Using this fact, an equation for $\dot{\sigma}_{\sigma\sigma}$ can be found and then $(\dot{\sigma}_T)_4$ and $(\dot{\sigma}_T)_3$ can be computed. Differentiating (3.11) with respect to yields

$$\bar{p}^{xy}_{\sigma}\dot{\sigma}_{\sigma\sigma} + \bar{m}^{xy}[\bar{u}^{xy}_{\sigma}\bar{p}^{y}_{\sigma x} + \bar{v}^{xy}\bar{p}^{x}_{\sigma y} + \bar{p}^{xy}_{\sigma}(\bar{u}^{y}_{\sigma x} + \bar{v}^{x}_{\sigma y})]$$

$$- \bar{p}^{xy}_{\sigma}(\bar{u}^{xy}_{\sigma}\bar{m}^{y}_{x} + \bar{v}^{xy}_{\sigma}\bar{m}^{x}_{y}) = 0 \quad . \tag{3.18}$$

After defining D_k as

$$D_k = -\left\{\frac{\bar{m}^{xy}}{\bar{p}^{xy}_{\sigma}}\,\bar{u}^{xy}_{\sigma}\bar{p}^{y}_{\sigma x} + \bar{v}^{xy}\bar{p}^{x}_{\sigma y} + \bar{p}^{xy}_{\sigma}(\bar{u}^{y}_{\sigma x} + \bar{v}^{x}_{\sigma y}) - (\bar{u}^{xy}_{\sigma}\bar{m}^{y}_{x} + \bar{v}^{xy}_{\sigma}\bar{m}^{x}_{y})\right\}_{k}, \tag{3.19}$$

then (3.19) can be written as

$$(\dot{\sigma}_T)_{k+1} + (\dot{\sigma}_T)_{k-1} - 2(\dot{\sigma}_T)_k = D_k \tag{3.20}$$

Applying (3.20) at levels k = 3 and 4 yields

$$\begin{aligned}(\dot{\sigma}_T)_5 + (\dot{\sigma}_T)_3 - 2(\dot{\sigma}_T)_4 &= \Delta\sigma^2 D_4 \\ (\dot{\sigma}_T)_4 + (\dot{\sigma}_T)_2 - 2(\dot{\sigma}_T)_3 &= \Delta\sigma^2 D_5\end{aligned} \tag{3.21}$$

Solving (3.21) for $(\dot{\sigma}_T)_3$ and $(\dot{\sigma}_T)_4$ given that

$$(\dot{\sigma}_T)_5 = \frac{(P_6 - P_5)}{(P_5 - P_2)}(\dot{\sigma}_B)_5 \tag{3.22}$$

and $(\dot{\sigma}_T)_2 = 0$ yields

$$(\dot{\sigma}_T)_4 = 1/3\,\{2(\dot{\sigma}_T)_5 - \Delta\sigma^2(2D_4 + D_3)\} \tag{3.23}$$

$$(\dot{\sigma}_T) = 1/3\,\{(\dot{\sigma}_T)_5 - \Delta\sigma^2(2D_3 + D_4)\} \tag{3.24}$$

Similarly, in the stratosphere

$$(\dot{\sigma}_S)_1 = -\tfrac{1}{8}\Delta\sigma^2 D_1 \tag{3.25}$$

where

$$(\dot{\sigma}_S)_0 = (\dot{\sigma}_S)_2 = 0 \quad . \tag{3.26}$$

3.4 Lateral Boundary Condition.

The 6L AWSPE has rigid impermeable walls between the two outermost grid rows (see Fig. 2.2). No heat or momentum is allowed to pass through the boundary, although flow parallel to the boundary is permitted. In finite-difference form these conditions may be written as:

$$\bar{u}^{x} = 0 \quad , \quad \theta_{x} = 0 \quad , \quad v_{x} = 0 \quad , \quad P_{\sigma x} = 0 \quad , \tag{3.27}$$

for x=constant

and for y = constant

$$u_{y} = 0 \quad , \quad \theta_{y} = 0 \quad , \quad \bar{v}^{y} = 0 \quad , \quad P_{\sigma y} = 0 \quad . \tag{3.28}$$

These conditions lead to the reflection of pure gravity waves at the boundaries.

3.5 Thermodynamic Forcing.

The eddy flux of heat from ocean surfaces is parameterized after the work of Lorenz (1962). The boundary layer is only heated if the sea surface temperature is greater than the boundary-layer potential temperature (θ). The 6L AWSPE model uses mean monthly sea surface temperature fields to derive the heating rate. The boundary-layer heating rate is given by

$$H = K \, (\overline{\theta - T_{w}})^{xy} \tag{3.29}$$

where $K = 10^{-4}$ s^{-1} and T_{w} is the sea surface temperature.

3.6 Horizontal Smoothing.

Explicit horizontal space smoothers are not used in the central portion of the model domain (north of 20N). Below 20N, two types of smoothers (tendency truncation and lateral diffusion) are used.

The tendency truncation is applied to the u, v, θ, and p_{σ} equations. This form of smoothing is used to reduce noise in the Tropical regions of the model. The model uses half of the computed tendency for the above variables below 10N and the full tendency at and above 20N. The two zones are blended linearly between 10N and 20N.

The lateral diffusion "smoother" is introduced into the u and v momentum equations as follows:

$$\frac{\partial u}{\partial t} = \text{(u tendency terms)} + \Delta \cdot (K \Delta u) \tag{3.30}$$

$$\frac{\partial v}{\partial t} = \text{(v tendency terms)} + \Delta\cdot(K\Delta v) \tag{3.31}$$

where

$$K = \begin{cases} 0 & ; \quad \phi > 20N \\ \frac{1}{2}[\sin(\phi_0 - \phi)\frac{90}{\Delta\phi} + 1]\ x10^6 m^2 s^{-1} & ; \quad 10N \leq \phi \leq 20N \\ 0 & ; \quad \phi < 10N \end{cases} . \tag{3.32}$$

3.7 Time Smoothing.

Because the model uses centered (leapfrog) time differencing, a time smoother is applied to control time splitting. The time smoother has the form:

$$\psi^{(n)^*} = \psi^n + (\psi^{(n-1)^*} - 2\psi^n + \psi^{n+1}) \tag{3.33}$$

where ψ represents the variables u, v, θ, and p_σ; n represents a given time level; and $\alpha = 0.075$ for even time steps and -0.075 for odd time steps.

3.8 Computation of Omega.

Omega (ω) is computed only for output for use by forecasters and other models. The model's vertical motion parameter is "sigma dot" (the total time rate of change of sigma) since the AWSPE model was formulated using sigma coordinates.

Omega is computed directly using

$$\omega = \frac{dp}{dt} = \frac{\partial p}{\partial t} + m(u\frac{\partial p}{\partial x} + v\frac{\partial p}{\partial y}) + \dot{\sigma}\frac{\partial p}{\partial \sigma} \tag{3.34}$$

or in finite difference form

$$\omega = \overline{p_t}^{t} + \overline{m}^{xy}(\overline{u}^{xy}\overline{p_x}^{y} + \overline{v}^{xy}\overline{p_y}^{x}) + \overline{(\dot{\sigma}\overline{p}^{xy})}^{xy}_{\sigma} . \tag{3.35}$$

The value of ω is then averaged over 2 h (6 time steps for which $\Delta t = 1200$ s) before output. For instance, the omega value "valid" at the 3-h forecast point would be an average of the values between forecast hour 1 and forecast hour 3.

3.9. Computation of the Geopotential Height.

The geopotential height for the 6L AWSPE is computed directly from the finite-difference formulation of the hydrostatic approximation. Eq. (3.9) is integrated in the vertical, given the terrain height, potential temperature, and pressure of the sigma levels. Values of Φ computed at the whole levels are averaged to the half levels where they are used in computing the u and v tendencies.

3.10. Dry Convective Adjustment.

The 6L AWSPE model applies a dry convective adjustment procedure to remove superadiabatic lapse rates and thus maintain model stability. Haltiner and Williams (1980) show that the phase speed of internal gravity waves is given by

$$c = \pm \frac{\mu}{\mu^2 + k^2} \left(\frac{g}{\bar{\theta}} \frac{\partial \theta}{\partial z} \right)^{\frac{1}{2}} \tag{3.36}$$

where μ and k are the wave numbers in x and z, respectively, g is gravity, and $\bar{\theta}$ is the mean value of the potential temperature using a standard perturbation analysis with

$$\theta = \bar{\theta}(z) + \theta'(x,z,t) \quad . \tag{3.37}$$

When the vertical lapse rate is superadiabatic, $\frac{\partial \bar{\theta}}{\partial z}$ becomes negative and the phase speed is complex. Thus, the internal gravity wave is unstable and will grow without bound; i.e. the model will become computationally unstable. Therefore, dry convective adjustment is applied in the model to adjust all superadiabatic lapse rates to the adiabatic or neutral position with $\frac{\partial \theta}{\partial z} = 0$.

4. THE 6-LAYER AWSPE MARCHING PROCESS.

The finite-difference equations are solved as follows:

a. Given initial values for u, v, θ, and p_σ ,the future values of these variables are computed using (3.7) through (3.11). In order to apply the pressure-gradient-averaging technique, the future values of p_σ and θ must be computed before the pressure-gradient force can be calculated. First $\dot{\sigma}$ is computed using the method given in Section 3.3. p_σ is now forecast from (3.11) and θ is computed using (3.10). Note that θ is not forecast in the isentropic top layer. Next, the pressure values at levels 0, 1, 2, 3, 4, 5,

and 6 for the future time step N+1 (where N represents an arbitrary time level or step) are computed by summing p_σ downward from the top level (-1) where p = 0.

b. Exner's function, π, at time step N+1 is computed from (2.6). Then (3.9) is used to compute the height fields, z, at levels 5 through -1 for time N+1 given the terrain field at level 6. The pressure-gradient force can be computed from the values of z, θ, and π at time steps N-1, N, N+1 using (3.7), (3.8), and (3.12).

c. Eqs. (3.7) and (3.8) are then solved for u and v at time step N+1.

This process is repeated in time until the desired forecast time is reached. For the first time step, the model uses forward differencing. After the first time step, a centered difference scheme is applied. Because the model uses pressure-gradient averaging a time step of 1200s is permitted.

5. INITIALIZATION

The initialization process is detailed in Shuman and Hovermale (1968). Currently, heights on pressure coordinates, taken from the AFGWC Hough Spectral Analysis Model (HUFANL), are interpolated to the 6L AWSPE sigma-coordinate domain using the temperature fields from the Hough Spectral Analysis Model (Tarbell and Hoke, 1979). These height values are then used to compute potential temperature, θ. The procedure uses a linear balance equation to compute the winds on the sigma domain given the height and potential temperature fields.

This balanced initialization procedure typically reduces the mass-weighted kinetic energy by about 10 to 15 percent when compared to the mass-weighted kinetic energy computed from the actual analysis.

6. OUTPUT FIELDS

The model forecast values on sigma surfaces are stored in a file on the computer every 3h of forecast time. A post processor interpolates the 3h sigma data on sigma surfaces to the AFGWC pressure-coordinate data base. This interpolation procedure computes the value of u, v, and T for the mandatory pressure levels by linear interpolation of the sigma-level values in Exner's function (π). The height field (z) at the sigma levels is computed from the hydrostatic equation. Then, the height and temperature fields are interpolated in π to mandatory pressure levels. The exact details of this procedure can be found in the 6L AWSPE Program Maintenance Manual (Andrew Johnson, 1975).

The pressure-coordinate data base is then stored in the AFGWC literal-label data base (under literal RTGWCF). This data base is used by display programs and other models.

This literal-label data base contains wind, temperature, and D-value fields in 3- to 6-h increments from the surface to 100 mb. Fields such as surface pressure, vorticity, vertical motion (omega), and tropopause height and temperature are carried at certain levels and times. Values are routinely forecast in the Northern Hemisphere to 72h for the 00 and 12 GMT data times and to 36h for the 06 and 18 GMT data times. Table 7.1 (from the AFGWC Data Base Handbook) lists the fields stored in the 6L AMSPE data base.

TABLE 6.1. 6L AMSPE Data Base

FIELD	Label	Level (LL) (mb*10)	Forecast Time (TT) (h)
D-value	TTAZLL	00	03, 06, ..., 24, 30, 36, 48, 60, 72
	TTAZLL	85, 70, 50, 40, 30, 25, 20, 15, 10	06, 12, ..., 48, 60, 72
	TTAZLL	50	96
Wind	TTAWLL	00	00, 03, 06, ..., 60
	TTAWLL	85, 70, 50, 30, 20, 10	00, 03, ..., 60, 72
	TTAWLL	40, 25, 15	06, 12, ..., 48, 60, 72
	TTAWLL	GR	09
Sfc Pres/ 1000mb Temp	TTAPLL	SF	03, 06, ..., 24, 30, 36
Vertical Velocity	TTADLL	70, 30, 10	00, 03, ..., 60
Stream Function	TTASLL	85, 70, 50, 30, 20, 10	00, 03, ..., 48
Tropopause Pres/Hgt/Temp	TTALLL	Tropopause	06, 12, ..., 48, 60, 72
Vorticity	TTAVLL	50	06, 12, ..., 48

7. DIFFERENCES BETWEEN THE 6-LAYER AWSPE MODEL AND THE NMC 7-LAYER SHUMAN-HOVERMALE PE MODEL

The 6L AWSPE is an early version of the 7-Layer Shuman-Hovermale PE model (7 LPE) used operationally at NMC until August 1980. The basic structure of the two models is very similar, but substantial differences do exist. In fact, the 7L PE forecasts verify substantially better than the 6L AWSPE forecasts.

Fig. 7.1 shows root-mean-square vector errors at 500 mb for the two models, the 1-bedient 6L AWSPE and the 1/2-bedient 7L PE for the period January 1979 to December 1980. One bedient is exactly equal to what we at AFGWC refer to as whole mesh, see Hoke, et.al. (1980) for further explanation. This figure clearly demonstrates the quality of the enhancements made by NMC to their version of the 1966 Shuman-Hovermale model.

We might ask why does the 1/2-bedient 7L PE verify better than the 6L AWSPE. Haltiner and Williams (1980) pointed out that reduced phase-speed error in the weather-producing waves leads to improved short-range forecasts for models like the 7L PE. They stated phase speed errors can be reduced by minimizing truncation errors. Thus, one of the most important reasons why the 6L AWSPE doesn't produce forecasts as good as the NMC 7L PE model is probably the reduced phase-speed errors due to the 1/2-bedient grid used by the NMC 7L PE. Less important reasons exist. For example, the 7L PE is a moist model that parameterizes latent heating effects. The 7L PE also uses a more sophisticated initialization technique.

8. A BRIEF DESCRIPTION OF THE SUBROUTINES IN THE 6-LAYER AWSPE PROGRAM

In this section, we will present a brief description of the different subroutines in the 6L AWSPE model taken from Johnson (1975). This section is intended for those requiring a more detailed knowledge of the 6L AWSPE.

Fig. 8.1 gives the 6-Layer AWSPE model subroutine flow diagram. The numbers in the lower-left hand corner of each subroutine give the order in which the programs are used. The basic function of each module shown in the diagram is defined below.

UTIME3 - The main routine for the 6L AWSPE forecast model. This routine controls all the forecast time steps and outputs all the forecast fields to mass storage.

STARTF - Initializes several of the constants used by the model.

FCST - Manages a single time step for the model forecast variables (i.e., wind, potential temperature and pressure of each sigma surface). To take advantage of the two central processors on the AFGWC UNIVAC 1110s, the 6L AWSPE model utilizes two separate activities to perform each forecast. Each activity forecasts half of the model domain for each variable.

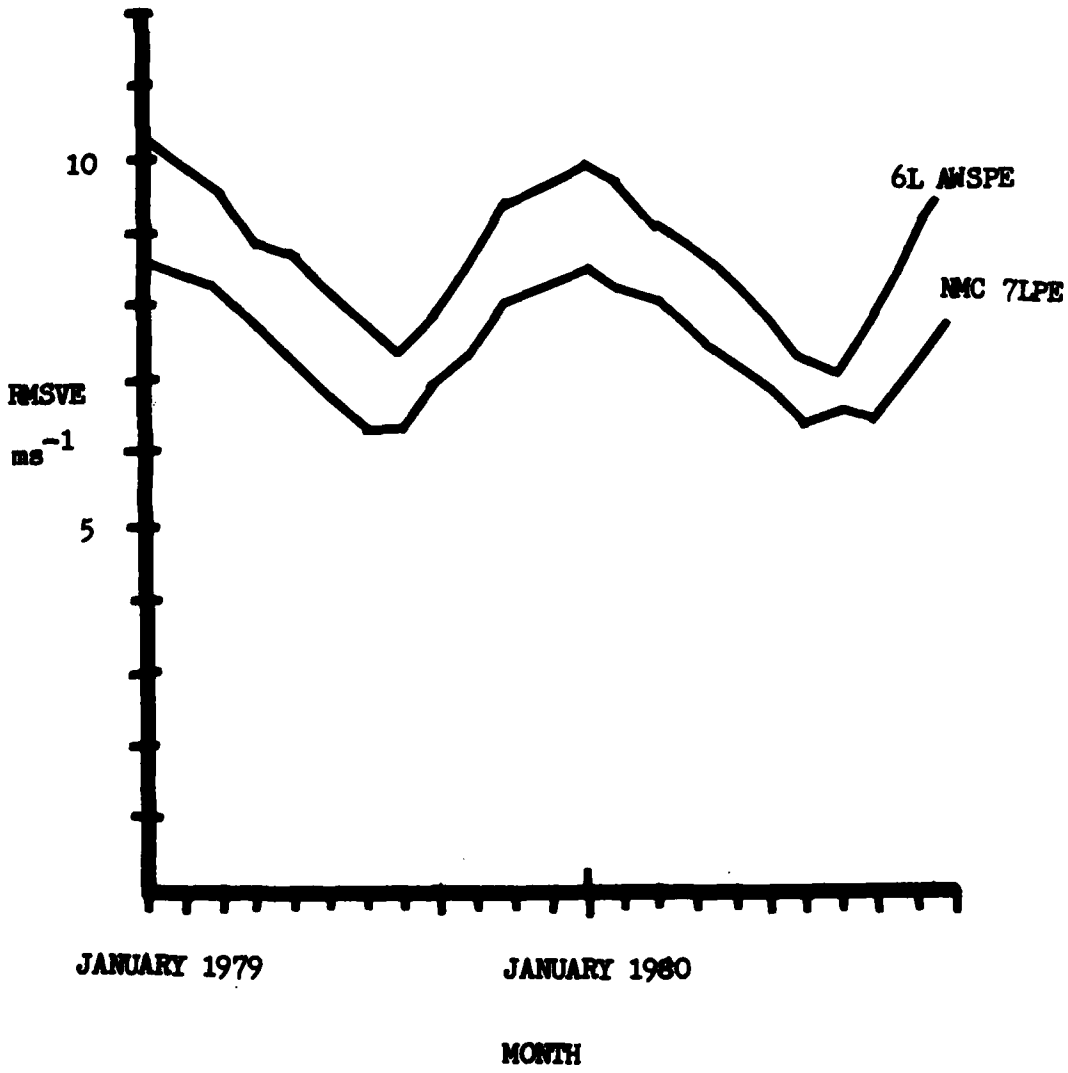

Figure 7.1. Objectively verified root-mean square vector errors for the 24h forecast at 500mb from January 1979 to December 1980 for the 6L AWSPE and NMC 7LPE.

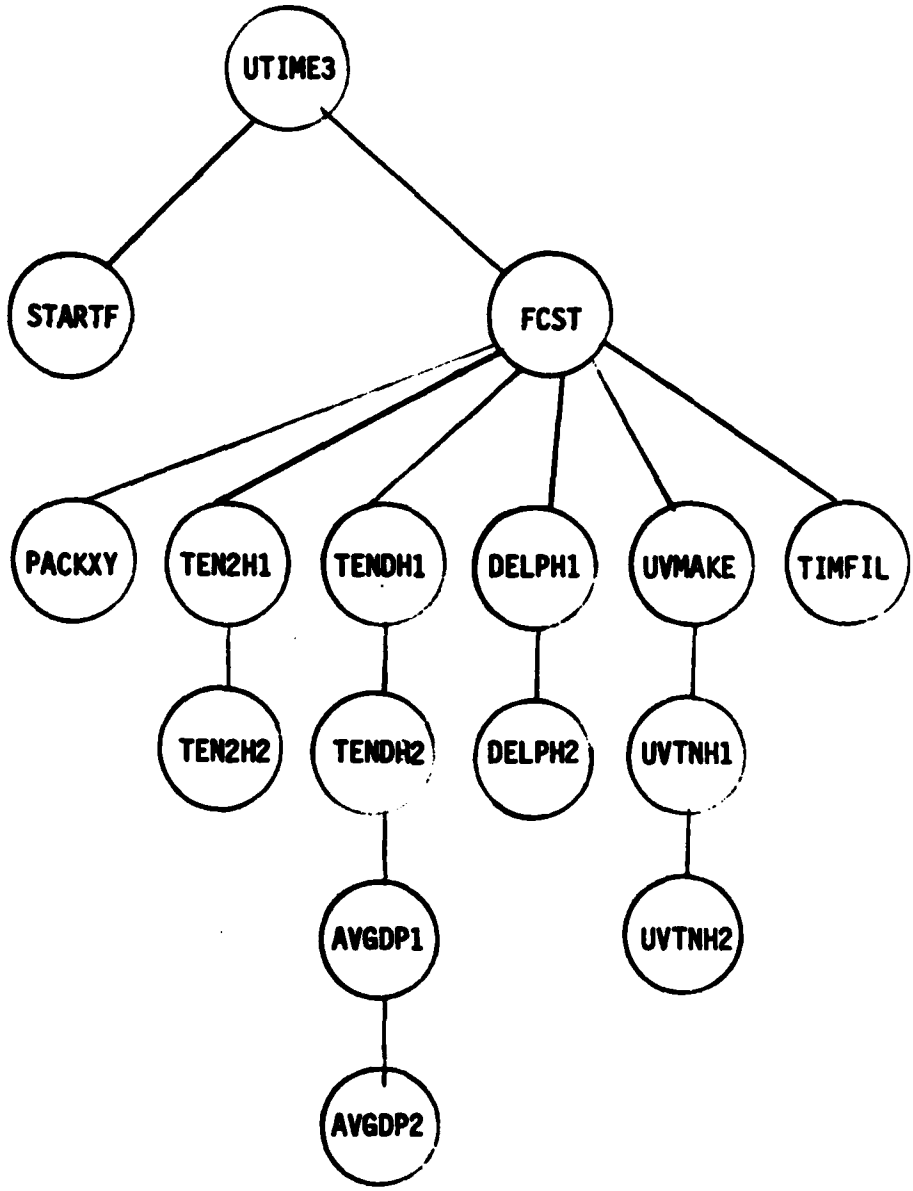

Figure 8.1. The 6L AWSPE Subroutine Flow Diagram

PACKXY - Packs or unpacks an input/output (I/O) buffer from or into the model forecast parameter arrays.

TENDH1 - This routine computes the tendency of the potential temperature (θ), the pressure thickness (p_σ), and the wind components (u , v) for the left half of the forecast domain.

TENDH2 - Same as TENDH1 except it acts on the right half of the forecast domain.

TEN2H1 - Computes the values at the next time step for θ and p_σ for the left half of the domain. It also computes the omega field.

TEN2H2 - Same as TEN2H1 except TEN2H2 acts on the right half of the forecast domain.

DELPH1 - Computes the pressure-gradient-force terms used to compute wind-vector tendencies for the left half of the model domain.

DELPH2 - Same as DELPH1 except DELPH2 acts on the right half of the model domain.

UVMAKE - Computes new horizontal wind components from the forecast wind tendencies.

TIMFIL - Performs a time smoothing of the forecast fields for the wind components, the pressure thickness fields, and the potential temperature.

AVGDP1 - Averages the pressure-gradient terms in time for the left half of the model domain.

AVGDP2 - Same as AVGDP1 except AVGDP2 acts on the right half of the model domain.

UVTNH1 - Adds the time-averaged pressure-gradient-force contributions to the horizontal wind component tendency equations for the left half of the model domain.

UVTHN2 - Same as UVTNH1 except UVTHN2 acts on the right half of the model domain.

The above routines apply the finite-difference equations given in Section 3 to produce the desired forecast. Thus, Fig. 8.1 really represents the high-level design of the 6L AWSPE model. The 6L AWSPE Maintenance Manual contains a more detailed explanation.

9. SUMMARY

We have presented the mathematical and numerical details of the 6L AWSPE model. We discussed the predecessor of the 6L AWSPE, the NMC 1966 6L

Shuman-Hovermale PE model. This model represented a major step forward in forecast accuracy when implemented at NMC in 1966 as well as when implemented at AFGWC in 1975.

Like its predecessor at NMC, the 6L ANSPE model uses the hydrostatic, sigma-coordinate, primitive equations on a polar stereographic projection of the earth. The finite-difference form of the equations is based on 2nd-order finite difference operators. The model domain consists of a rectangular area centered on the North Pole. At the boundary (near 10N), the model uses an isothermal, no-slip boundary condition. Terrain is included in the model by virtue of the sigma coordinate system. Time and space smoothing are used to control space and temporal noise. Ocean boundary-layer heat flux is parameterized. Surface drag is applied in the lowest layer, and pressure-gradient averaging is used to allow a longer time step.

To initialize the model, analyzed heights are interpolated linearly in Exner's function from a pressure- to a sigma-coordinate system. The potential temperatures at the sigma levels are computed. Winds are calculated using a linear balance relationship. The model forecasts on the sigma domain starting from the initial conditions using a centered-time-differencing scheme. The forecast length is normally 72 h for 00 and 12 GMT data times and 36 h for the 06 and 18 GMT data times. The forecast fields on sigma surfaces are interpolated and stored in the AFGWC pressure-coordinate data base. The forecast fields of temperature, wind, height, and other parameters are available for use by other computer programs.

PART II: The 7-Layer AWSPE Model

Captain Fred P. Lewis
Major Terry C. Tarbell
First Lieutenant Larry G. Renninger
First Lieutenant Allan M. Weiner

10. INTRODUCTION

Before discussing the 7-Layer AWSPE model, we will discuss the problems that led to the model's development. We will then present some of the advantages of the model as compared to the 6-layer version.

Since its implementation in 1975 the 6L AWSPE program has run on AFGWC's System V. However, System V is dedicated to satellite data processing. By late 1979, System V had become overloaded with satellite data. At that time, we proposed moving the 6L AWSPE to the meteorological models and applications computer, System I, to help alleviate this saturation problem.

AFGWC personnel believed after a new UNIVAC 1100/81 computer was installed as System I, it would be possible to move the 6L AWSPE to System I. After several tests, we demonstrated that the vast amount of I/O time required by the 6L AWSPE made it impossible for the model to meet required timelines on the new System I. This I/O time is required because the model works on only 3 vertical strips at a time. System I has a more powerful CPU than System V, but the I/O processing unit is not as efficient. Thus, AFGWC decided to develop an entirely core-contained version of the Shuman-Hovermale PE model that required few I/O operations, thereby permitting a faster runtime on System I.

Improvements made to the Shuman-Hovermale model at NMC during the 1970's led TSIN to develop a core-contained version of the NMC 7L PE rather than a core-contained version of the 6L AWSPE. As stated in Part I, the 6L AWSPE is a dry version of the original 1966 Shuman-Hovermale 6L PE model. Some modifications were made during the mid 1970's to the 6L AWSPE to allow a longer time step: pressure-gradient averaging, tendency truncation south of 20N, and horizontal space smoothing. These changes did not significantly improve forecast accuracy. Thus, AFGWC forecasters and others (e.g., Leary, 1971) continued to identify problem areas in the 6L AWSPE forecasts. Two examples are the slow phase speed of the shorter, weather producing waves and the generation of spurious vorticity patterns near the model boundaries. NMC solved both of these problem areas in the 7L PE model by incorporating better physical and numerical techniques.

To remedy some of the 6L AWSPE model disadvantages and to efficiently take advantage of the large memory available (1,000,000 words) on System I, AFGWC decided to develop 2nd- and 4th-order core contained versions of the NMC 7L PE developed by Campana (1977, 1978, 1979a, and 1979b). AFGWC/DO tasked TSIN with this technology transfer project. The large amount of memory this model uses (400,000 words) eliminates 90 percent of all I/O operations and should allow the 7L AWSPE to run operationally on System I. Furthermore, the improved numerical forecast techniques (4th order differencing and better boundary conditions) will definitely improve the model forecasts.

10.1 The 7-Layer AWSPE Model.

When comparing the 7L and 6L AWSPE models, the major improvements in the 7L version lie in the more sophisticated numerical techniques used. The specific techniques are listed below.

(1) The 7L AWSPE has the capability to use 4th-order finite differencing for the advection terms in the equations of motion. Campana (1978) showed that the 1-bedient grid version of the NMC 7L PE model with 4th-order finite differencing verifies nearly as accurately as the 2nd-order, 1/2-bedient version. Both the 4th-order, 1-bedient and 2nd-order, 1/2-bedient models produce better forecasts because they handle the propagation speeds of the shorter weather producing waves more accurately than a 1-bedient, 2nd-order model. The computer cost of a 1/2-bedient model is approximately 8 times greater than for a 1-bedient model, while only about a 40 percent cost increase is involved in going from 2nd- to 4th-order finite differencing at the same grid increment. Campana (1978) showed that 4th-order differencing was a very cost-effective way to improve numerical forecasts.

(2) The 7L AWSPE uses the "energy-vorticity" form for the equations of motion while the 6L AWSPE uses the "standard" u and v wind component form of the equations of motion. Shuman and Stackpole (1968) showed that the finite-difference form of the "standard" set of equations leads to spurious vorticity production, while the "energy-vorticity" finite-difference form does not. Forecasters also have noticed a significant amount of spurious vorticity generated at the boundaries in the current 6L AWSPE model.

(3) The 7L AWSPE forecasts winds and potential temperatures at 7 layers in the model atmosphere. The 6L AWSPE forecasts the wind and potential temperature for 6 layers. NMC has found that by making the additional layer an active forecast layer, model verification improves slightly in the upper layers.

(4) The 7L AWSPE uses energy-conserving finite-difference schemes for computing geopotential heights from the hydrostatic equation and for applying dry convective adjustment. Arakawa's (1972) energy-conserving scheme, as given by Phillips (1974), is used to compute the geopotential height.

(5) Other differences between the 6L and 7L AWSPE models do exist. These will be covered by the more detailed description of the 7L AWSPE model given in the following sections. Section 11 will cover the model

primitive equations, while Section 12 will present the finite-difference formulation of the 7L AWSPE. The marching process will be outlined in Section 13. Sections 14 and 15 will discuss the initialization and output fields, respectively. In Section 16 we will present the 7L AWSPE model flow diagram and abridged maintenance manual.

11. THE 7-LAYER ASWPE MODEL CHARACTERISTICS

11.1 The Primitive Equations.

Campana (1978) presented the energy-vorticity form of the hydrostatic meteorological equations for a model with a vertical sigma coordinate and horizontal Cartesian coordinates on a conformal polar stereographic projection of the earth as:

$$\frac{\partial u}{\partial t} = v\left[f + m^2\left(\frac{\partial v}{\partial x} - \frac{\partial u}{\partial y}\right)\right] - \frac{\partial E}{\partial x} - \widetilde{\left[\frac{\partial \phi}{\partial x} + c_p\theta\frac{\partial \pi}{\partial x}\right]} - \dot{\sigma}\frac{\partial u}{\partial \sigma} + F_x \tag{11.1}$$

$$\frac{\partial v}{\partial t} = -u\left[f + m^2\left(\frac{\partial v}{\partial x} - \frac{\partial u}{\partial y}\right)\right] - \frac{\partial E}{\partial y} - \widetilde{\left[\frac{\partial \phi}{\partial y} + c_p\theta\frac{\partial \pi}{\partial y}\right]} - \dot{\sigma}\frac{\partial v}{\partial \sigma} + F_y \tag{11.2}$$

$$\frac{\partial \theta}{\partial t} = -m^2\left(u\frac{\partial \theta}{\partial x} + v\frac{\partial \theta}{\partial y}\right) - \dot{\sigma}\frac{\partial \theta}{\partial \sigma} + Q \tag{11.3}$$

$$\frac{\partial \phi}{\partial \sigma} + c_p\theta\frac{\partial \pi}{\partial \sigma} = 0 \tag{11.4}$$

$$\frac{\partial p_\sigma}{\partial t} = -m^2\left[\bar{u}\frac{\partial p_\sigma}{\partial x} + \bar{v}\frac{\partial p_\sigma}{\partial y} + p_\sigma\overline{\left(\frac{\partial u}{\partial x} + \frac{\partial v}{\partial y}\right)}\right] - \varepsilon(\dot{\sigma}_B)_2 p_{\sigma_B} \tag{11.5}$$

$$\varepsilon = \begin{cases} 0 & \text{statosphere and boundary layer} \\ 1 & \text{troposphere} \end{cases}$$

where E is defined as:

$$E = \tfrac{1}{2}(u_0^2 + v_0^2)^{\frac{1}{2}} \tag{11.6}$$

where

$$u_0 = um, \quad v_0 = vm \quad . \tag{11.7}$$

These six equations are written in the six dependent variables u, v, θ, π, Φ, and p_σ. The variables, u and v, are the horizontal wind components, θ is the potential temperature, f is the Coriolis parameter, m is the map factor, Φ is the geopotential height, p_σ is the pressure thickness between the three sigma domains; and π is Exner's function. Q represents heating and for the current version Q represents only the sea surface heat flux. F represents friction which is only used in the 7L AWSPE in the form of surface drag. The overriding bar, $\overline{(\quad)}$, in (11.5) represents a vertical average within each sigma domain. The $\widetilde{(\quad)}$ in (11.1) and (11.2) represents the pressure gradient averaging technique given by Brown and Campana (1978).

11.2 The Vertical Domain.

Fig. 11.1 is a depiction of the vertical structure of the 7L AWSPE model. The model contains seven vertical layers which are partitioned into three separate sigma domains. The lowest layer is a planetary boundary layer with the vertical coordinate defined by

$$\sigma_B = \frac{p-p_0}{p_7^*-p_6} \quad . \tag{11.8}$$

The second sigma domain consists of three layers and covers the remainder of the troposphere. This domain is defined by

$$\sigma_T = \frac{p-p_3^{**}}{(p_7-50)-p_3^{**}} \tag{11.9}$$

where p^{**} is the pressure at the tropopause. The tropopause is considered to be a material surface; i.e., $\dot{\sigma}_3 = 0$.

The third sigma domain consists of three layers and constitutes the model stratosphere. The stratospheric domain is defined by

$$\sigma_S = \frac{p-p_0}{p_3^{**}-p_0} \quad . \tag{11.10}$$

The top of the model is specified at p = 50 mb.

11.3 The Horizontal Grid.

The 7L AWSPE uses the horizontal grid described in Section 2.3.

11.4 Prognostic and Diagnostic Variables.

The forecast or history variables are u, v, p_σ, and θ . The diagnosed variables are π , z, $\dot{\sigma}$, and p. In Fig. 11.1, we show that u, v, z, p and π are defined at the half levels and $\dot{\sigma}$ and p are defined at the full levels. Actually, $\dot{\sigma}$ is defined at the center point of each square formed by four full-level grid points (see Fig. 11.2). The methods used to calculate these variables will be presented in the next two sections.

12. SECOND- AND FOURTH-ORDER FINITE-DIFFERENCE FORMULATION OF THE 7-LAYER AWSPE MODEL.

In this section, we present the second and fourth-order finite-difference formulations of the model, the parameterization of planetary boundary layer (PBL) friction, the method of calculation of $\dot{\sigma}$, the lateral boundary conditions, the horizontal smoothing, the time smoothing, the pressure-gradient-averaging methods, and the technique used to compute ω .

12.1 The 7-Layer Second- and Fourth-Order AWSPE Finite-Difference Equations.

Again, we will use the shorthand notation given in Part I (Shuman and Hovermale, 1968). The operator used to construct the second-order version (i.e., $\bar{f}^x$ and f_x) will remain the same. Campana (1977 introduced the fourth-order operators using similar notation. He defines f_{xh} and $\bar{f}^{xh}$ to be fourth-order operators for the derivative and the sum as:

$$f_{x_h} = {}^9/_8\left(\frac{f_{i+1/2} - f_{i-1/2}}{\Delta x}\right) - {}^1/_8\left(\frac{f_{i+3/2} - f_{i-3/2}}{3\Delta x}\right) \tag{12.1}$$

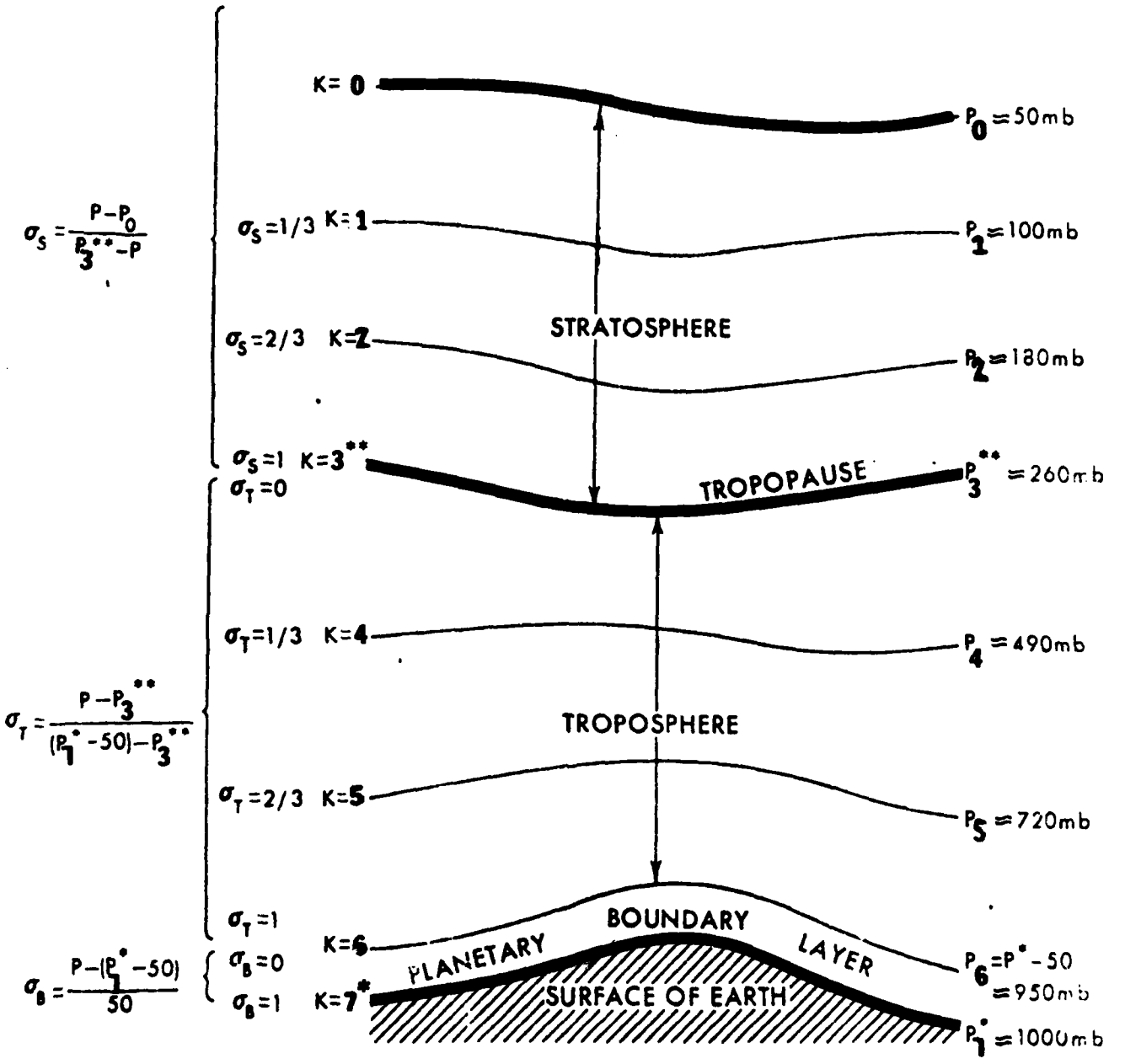

Figure 11.1. Depiction of the vertical structure of the 7L AWSPE model.

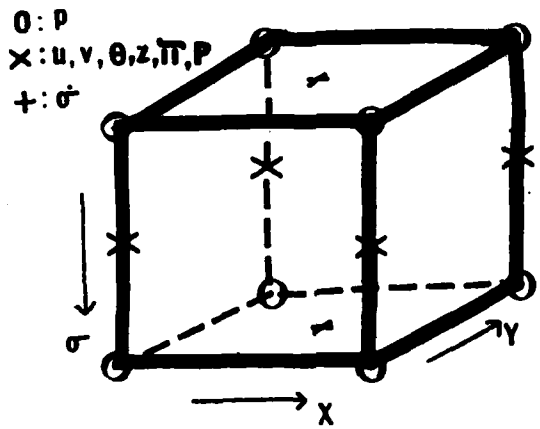

Figure 11.2. Schematic box connecting eight adjacent grid points, after Shuman and Hovermale (1968).

$$\overline{f}^{xh} = 9/8\left(\frac{f_{i+1/2} + f_{i-1/2}}{2}\right) - 1/8\left(\frac{f_{i+3/2} + f_{i-3/2}}{2}\right) \tag{12.2}$$

As in the second-order formulation, the derivative and averaging operator are valid midway between a set of four grid points. Thus, the derivative is used to go to the half grid points and the sum is used to return to the whole grid point.

Now define the fourth-order operators for the horizontal. First, it is instructive to define the second-order operators for comparison purposes. These operators for a horizontal (x,y) coordinate system are given by:

$$\overline{f}_x^y = \frac{1}{2\Delta x}\left(f_{i+1/2,j+1/2} - f_{i-1/2,j+1/2} + f_{i+1/2,j-1/2} - f_{i-1/2,j-1/2}\right) \tag{12.3}$$

$$\overline{f}_y^x = \frac{1}{2\Delta x}\left(f_{i+1/2,j+1/2} - f_{i+1/2,j-1/2} + f_{i-1/2,j+1/2} - f_{i-1/2,j-1/2}\right) \tag{12.4}$$

$$\overline{f}^{xy} = 1/4\left(f_{i+1/2,j+1/2} + f_{i+1/2,j-1/2} + f_{i-1/2,j-1/2} + f_{i-1/2,j+1/2}\right) \tag{12.5}$$

where i refers to grid points in the x-direction and j refers to grid points in the y-direction. The fourth-order operators are found by combining (12.1) and (12.2). For a horizontal (x,y) coordinate system, these operators are given by

$$\begin{aligned}\overline{f}_{x_h}^{y_h} = \frac{1}{384\Delta x}\Big[&243\left(f_{i+1/2,j+1/2} - f_{i-1/2,j+1/2} + f_{i+1/2,j-1/2} - f_{i-1/2,j-1/2}\right)\\ &- 27\left(f_{i+1/2,j+3/2} - f_{i-1/2,j+3/2} + f_{i+1/2,j-3/2} - f_{i-1/2,j-3/2}\right)\\ &- 9\left(f_{i+3/2,j+1/2} - f_{i-3/2,j+1/2} + f_{i+3/2,j-1/2} - f_{i-3/2,j-1/2}\right)\\ &+ \left(f_{i+3/2,j+3/2} - f_{i-3/2,j+3/2} + f_{i+3/2,j-3/2} - f_{i-3/2,j-3/2}\right)\Big]\end{aligned} \tag{12.6}$$

$$\overline{f}^{x_h}_{y_h} = \frac{1}{384\Delta x}\Big[243\left(f_{i+\frac{1}{2},j+\frac{1}{2}} - f_{i+\frac{1}{2},j-\frac{1}{2}} + f_{i-\frac{1}{2},j+\frac{1}{2}} - f_{i-\frac{1}{2},j-\frac{1}{2}}\right) \tag{12.7}$$

$$- 27\left(f_{i+3/2,j+\frac{1}{2}} - f_{i+3/2,j-\frac{1}{2}} + f_{i-3/2,j+\frac{1}{2}} - f_{i-3/2,j-\frac{1}{2}}\right)$$

$$- 9\left(f_{i+\frac{1}{2},j+3/2} - f_{i+\frac{1}{2},j-3/2} + f_{i-\frac{1}{2},j+3/2} - f_{i-\frac{1}{2},j-3/2}\right)$$

$$+ \left(f_{i+3/2,j+3/2} - f_{i+3/2,j-3/2} + f_{i-3/2,j+3/2} - f_{i-3/2,j-3/2}\right)\Big]$$

$$\overline{f}^{x_h y_h} = \frac{1}{256}\Big[81\left(f_{i+\frac{1}{2},j+\frac{1}{2}} + f_{i+\frac{1}{2},j-\frac{1}{2}} + f_{i-\frac{1}{2},j+\frac{1}{2}} + f_{i-\frac{1}{2},j-\frac{1}{2}}\right) \tag{12.8}$$

$$- 9\left(f_{i+3/2,j+\frac{1}{2}} + f_{i+3/2,j-\frac{1}{2}} + f_{i-3/2,j+\frac{1}{2}} + f_{i-3/2,j-\frac{1}{2}}\right.$$

$$\left. + f_{i+\frac{1}{2},j+3/2} + f_{i+\frac{1}{2},j-3/2} + f_{i-\frac{1}{2},j+3/2} + f_{i-\frac{1}{2},j-3/2}\right)$$

$$+ \left(f_{i+3/2,j+3/2} + f_{i+3/2,j-3/2} + f_{i-3/2,j+3/2} + f_{i-3/2,j-3/2}\right)\Big]$$

These fourth-order operators require many more calculations than the comparable second-order ones given by (12.3) through (12.5).

Next, we present the second- and fourth-order versions of the 7L ANSPE. Campana (1978) found that equally accurate forecasts could be obtained either by (1) using the fourth-order operators for the non linear advection terms and final overbar operation only or by (2) using the fourth-order operators for every operation. Therefore, the fourth-order version we developed uses fourth-order differencing only for the nonlinear advection terms and the final overbar operation.

Using the Shuman-Hovermale finite-difference notation and neglecting heating and friction, the finite-difference representations of (11.1) through (11.5) for the second-order finite-difference model can be written (Campana, 1978):

$$\frac{\partial u}{\partial t} = \overline{\bar{v}^{xy}\left[\bar{f}^{xy} + \overline{m^2}^{xy}\left(\bar{v}^{y}_{x} - \bar{u}^{x}_{y}\right)\right]}^{xy} - \bar{E}^{y}_{x} - \left[\widetilde{\bar{\phi}^{y}_{x} + c_p\bar{\theta}^{xy}\bar{\pi}^{y}_{x}}\right] - \overline{\left(\dot{\sigma}\,\bar{u}_{\sigma}\right)}^{\sigma} \qquad (12.9)$$

$$\frac{\partial v}{\partial t} = -\overline{\bar{u}^{xy}\left[\bar{f}^{xy} + \overline{m^2}^{xy}\left(\bar{v}^{y}_{x} - \bar{u}^{x}_{y}\right)\right]}^{xy} - \bar{E}^{x}_{y} - \left[\widetilde{\bar{\phi}^{x}_{y} + c_p\bar{\theta}^{xy}\bar{\pi}^{x}_{y}}\right] - \overline{\left(\dot{\sigma}\bar{v}_{\sigma}\right)}^{\sigma} \qquad (12.10)$$

$$\frac{\partial \theta}{\partial t} = -\overline{m^2}^{xy}\left(\bar{u}^{xy}\,\bar{\theta}^{y}_{x} + \bar{v}^{xy}\bar{\theta}^{x}_{y}\right) - \overline{\left(\dot{\sigma}\,\bar{\theta}^{xy}_{\sigma}\right)}^{\sigma} \qquad (12.11)$$

$$\frac{\partial p_\sigma}{\partial t} = -\overline{m^2}^{xy}\left[\overline{U^{xy}p^{y}_{\sigma x}} + \overline{V^{xy}p^{x}_{\sigma y}} + \overline{p^{xy}_{\sigma}\left(\bar{u}^{y}_{x} + \bar{v}^{x}_{y}\right)}\right] - \varepsilon(\dot{\sigma}_T)\,\delta\bar{p}^{xy}_{\sigma_T} \qquad (12.12)$$

where $U = \bar{u}$; $V = \bar{v}$; $\overline{(\;)} = \int_\sigma (\;)\,d\sigma$.

The $\widetilde{(\;)}$ over the pressure-gradient-force terms in (12.9) and (12.10) represents the pressure-gradient-averaging technique of Brown and Campana (1978).

The corresponding fourth-order equations are written as:

$$\frac{\partial u}{\partial t} = \overline{\bar{v}^{xy}\left[\bar{f}^{xy} + \overline{m^2}^{xy}\left(\bar{v}^{y}_{x_h y_h} - \bar{u}^{x}_{y_h}\right)\right]}^{x_h y_h} - \bar{E}^{y}_{x_h} - \left[\widetilde{\bar{\phi}^{y}_{x} + c_p\bar{\theta}^{xy}\bar{\pi}^{y}_{x}}\right] - \overline{\left(\dot{\sigma}\,\bar{u}_{\sigma}\right)}^{\sigma} \qquad (12.13)$$

$$\frac{\partial v}{\partial t} = -\overline{\bar{u}^{xy}\left[\bar{f}^{xy} + \overline{m^2}^{xy}\left(\bar{v}^{y}_{x_h y_h} - \bar{u}^{x}_{y_h}\right)\right]}^{x_h y_h} - \bar{E}^{x}_{y_h} - \left[\widetilde{\bar{\phi}^{x}_{y} + c_p\bar{\theta}^{xy}\bar{\pi}^{x}_{y}}\right] - \overline{\left(\dot{\sigma}\bar{v}_{\sigma}\right)}^{\sigma} \qquad (12.14)$$

$$\frac{\partial \theta}{\partial t} = -\overline{m^2}^{xy}\left(\overline{u}^{xy}\overline{\theta}^{y}_{x_h} - \overline{(\dot{\sigma}\bar{\theta}^{xy})}^{\sigma}\right)^{x_h y_h} \tag{12.15}$$

$$\frac{\partial p_\sigma}{\partial t} = -\overline{m^2}^{xy}\left[\overline{U}^{xy}\overline{p_\sigma}^{y}_{x_h} + \overline{V}^{xy}\overline{p_\sigma}^{x}_{y_h} + p_\sigma(\overline{U}^{y}_{x}+\overline{V}^{x}_{y})\right] - \varepsilon(\dot{\sigma}_T)_6\overline{p}^{xy}_{\sigma_T}{}^{xy} \tag{12.16}$$

where $U = \bar{u}$; $V = \bar{v}$; $\overline{(\ )} = \int_\sigma (\ )\,d\sigma$.

Note, as stated before, fourth-order differencing is used only for the nonlinear advection terms and for the final averaging (final overbar) operation.

12.2 PBL Friction.

For the 7L AWSPE, frictional dissipation is considered only in the model boundary layer. The formulation of this frictional dissipation is the same as given in Part I, Section 3.2.

12.3 The Calculation of "Sigma Dot".

In a manner similar to the 6L AWSPE model, the method used to compute $\dot{\sigma}$ for the 7L AWSPE follows almost directly from the finite-difference form of the p_σ tendency equation (3.11) and the fact that $\dot{\sigma} = 0$ at levels $\kappa = 7^*$, 3^{**}, and 0.

First, $p_\sigma = 50$ mb in the boundary layer and is constant in time and space. Thus, if we use the non-vertically integrated form of (12.16) and remove the $\overline{(\ \ )}^{xy}$, we have

$$\overline{p_\sigma}^{t} = 0 = -\overline{m^2}^{xy}\left(\overline{u}^{xy}\overline{p_\sigma}^{y}_{x} + \overline{v}^{xy}\overline{p_\sigma}^{x}_{y} + \overline{p_\sigma}^{xy}(\overline{u}^{y}_{x} + \overline{v}^{x}_{y}) - \overline{p_\sigma}^{xy}\dot{\sigma}_\sigma\right) \tag{12.17}$$

but

$$(\dot{\sigma}_B)_6 = \frac{(\dot{\sigma}_B)_7 - (\dot{\sigma}_B)_6}{\Delta\sigma} = -(\dot{\sigma}_B)_6 \tag{12.18}$$

where

$$(\sigma_B)_7 = 0 \; ; \qquad \Delta\sigma = 1 \tag{12.19}$$

and

$$(\dot{\sigma}_B)_6 = \overline{m^2}^{xy} \, (\overline{u}^y_x + \overline{v}^x_y) \tag{12.20}$$

A different approach must be employed in the troposphere since p_σ varies both in time and space. However, p_σ is linear with respect to σ. Therefore $p_{\sigma\sigma}$ is equal to zero. Using this fact, an equation for $\dot{\sigma}_{\sigma\sigma}$ can be found and then $(\dot{\sigma}_T)_5$ and $(\dot{\sigma}_T)_4$ can be computed. Differentiating (3.11) with respect to σ yields

$$\overline{p}^{xy}_\sigma \dot{\sigma}_{\sigma\sigma} + \overline{m^2}^{xy} \, [\overline{u}^{xy}_\sigma \overline{p}^{y}_{\sigma x} + \overline{v}^{xy}_\sigma \overline{p}^{y}_{\sigma x} + \overline{p}^{xy}_\sigma (\overline{u}^y_{\sigma x} + \overline{v}^x_{\sigma y})] = 0 \quad . \tag{12.21}$$

Thus defining

$$D_k = -\left\{ \frac{\overline{m^2}^{xy}}{\overline{p}^{xy}_\sigma} \, [\overline{u}^{xy}_\sigma \overline{p}^{y}_{\sigma x} + \overline{v}^{xy}_\sigma \overline{p}^{y}_{\sigma x} + \overline{p}^{xy}_\sigma (\overline{u}^y_{\sigma x} + \overline{v}^x_{\sigma y})] \right\}_k \tag{12.22}$$

(12.21) can be written as

$$(\dot{\sigma}_T)_{k+1} + (\dot{\sigma}_T)_{k-1} - 2(\dot{\sigma}_T)_k = \Delta\sigma^2 D_k \quad . \tag{12.23}$$

Applying (12.23) at levels k = 5 and 4 yields

$$(\dot{\sigma}_T)_6 + (\dot{\sigma}_T)_4 - 2(\dot{\sigma}_T)_5 = \Delta\sigma^2 D_5$$

$$(\dot{\sigma}_T)_6 + (\dot{\sigma}_T)_4 = 2(\dot{\sigma}_T)_5 = \Delta\sigma^2 D_5 \qquad (12.24)$$

Solving (12.24) for $(\dot{\sigma}_T)_4$ and $(\dot{\sigma}_T)_5$ and given that

$$(\dot{\sigma}_T)_6 = \frac{p_7 - p_6}{p_6 - p_3}(\dot{\sigma}_B)_6 \qquad (12.25)$$

and $(\dot{\sigma}_T)_3 = 0$ yields

$$(\dot{\sigma}_T)_5 = {}^1/_3\left\{[2(\dot{\sigma}_T)_6 - \Delta\sigma^2(2D_5 + D_4)]\right\} \qquad (12.26)$$

$$(\dot{\sigma}_T)_4 = {}^1/_3\left\{[(\dot{\sigma}_T)_6 - \Delta\sigma^2(2D_4 + D_5)]\right\} \qquad (12.27)$$

Similarly, in the stratosphere

$$\dot{\sigma}_1 - 2\dot{\sigma}_2 = \Delta\sigma^2 D_2$$

$$\dot{\sigma}_2 - 2\dot{\sigma}_1 = \Delta\sigma^2 D_1 \qquad (12.28)$$

Thus

$$\delta_2 = -\frac{\Delta\sigma^2}{3}(2D_2 + D_1)$$
$$\delta_1 = -\frac{\Delta\sigma^2}{3}(D_2 + 2D_1) \qquad (12.29)$$

12.4 Lateral Boundary Conditions.

The 7L AWSPE has the capability to use either the no-slip boundary conditions described in Section 3.4, or the sponge boundary conditions developed by Deaven at NMC in 1979. We will outline the sponge boundary conditions (NMC Numerical Weather Prediction Activities Report, 1979).

The sponge boundary is designed to provide a better forecast near the outer edges of the model domain by damping waves traveling toward or away from the boundary. To damp these waves, the following term is added to the u, v, θ, and p_σ tendency equations at the second through sixth grid rows from the boundary:

$$K[\phi^{t-1}_{i+1,j} + \phi^{t-1}_{i-1,j} + \phi^{t-1}_{i,j+1} + \phi^{t-1}_{i,j-1} - 4\phi^{t-1}_{i,j} - (\phi^{0}_{i+1,j} + \phi^{0}_{i-1,j} + \phi^{0}_{i,j+1} + \phi^{0}_{i,j-1} - 4\phi^{0}_{i,j})] \qquad (12.30)$$

where Φ represents u, v, p_σ and θ ; Φ^o is the value at the initial time; and K is 0.04 for the 7L AWSPE. The value at the boundary (grid row 1) is maintained at the initial value throughout the forecast period. Thus, the rows near the boundary are continually nudged towards the initial boundary values.

12.5 Thermodynamic Forcing

Thermodynamic forcing in 7L AWSPE model is the same as the 6L AWSPE (Part I, Section 3.5). As before, the only forcing is due to the eddy flux of heat from the ocean surface.

12.6 Horizontal Smoothing.

The 7L AWSPE model can use two additional forms of smoothing besides the smoothing included in the finite-difference formulation of the model. The first, which is always used, is the diffusive space smoother given by Shuman (1977). The plan of this smoother is

$$\begin{pmatrix} \frac{1}{4}(1-\mu)^2 & \frac{1}{2}\mu(1-\mu) & \frac{1}{4}(1-\mu)^2 \\ \frac{1}{2}\mu(1-\mu) & \mu^2-1 & \frac{1}{2}\mu(1-\mu) \\ \frac{1}{4}(1-\mu)^2 & \frac{1}{2}\mu(1-\mu) & \frac{1}{4}(1-\mu)^2 \end{pmatrix} \qquad (12.31)$$

where μ is chosen as 0.98 for the 7L AWSPE. That is, each variable is smoothed by applying the above plan at each grid point. The weight at the central grid point where the smoothing result is added to the original value is given by μ^2-1 . Other weights are as specified in the plan.

The second form is applied below 20N. This smoother is the tendency truncation is given in Section 3.6 of Part I.

12.7 Time Smoothing.

Because the model uses leapfrog time differencing scheme, a time smoother is applied to control time splitting. The time smoother has the form:

$$\psi^{(n)*} = \psi^n + \alpha(\psi^{(n-1)*} - 2\psi^n + \psi^{n+1}) \qquad (12.32)$$

where ψ represents the variables u, v, θ, and p_σ , n represents a given time level, and $\alpha = 0.075$.

12.8 Computation of Omega

Omega (ω) is diagnosed for use by forecasters and applications programs. The model does not use the ω value in any way. "Sigma dot" ($\dot{\sigma}$) is the model's vertical motion parameter.

is computed directly using

$$\omega = \frac{dp}{dt} = \frac{\partial p}{\partial t} + u\frac{\partial p}{\partial x} + v\frac{\partial p}{\partial y} + \dot{\sigma}\frac{\partial p}{\partial \sigma}$$

or in finite difference form

$$\omega = \overline{p}^{t}_{t} + \overline{m}^{xy}\left(\overline{u}^{xy}\overline{p}^{y}_{x} + \overline{v}^{xy}\overline{p}^{x}_{y}\right) + \overline{(\dot{\sigma}p)}^{xy}_{\sigma} \quad . \tag{12.33}$$

The value of ω is then averaged over a 2-h period (6 time steps for which $\Delta t = 1200$ s) before output. For instance, the value "valid" at the 3-h forecast point would be an average from 1+20 to 3+20.

12.9 Computation of the Geopotential Height

Unlike the 6L AWSPE, the 7L AWSPE does not use the simple finite-difference form of the hydrostatic equation (i.e. (3.9)) used by the 6L AWSPE to compute the geopotential height. Instead the 7L AWSPE uses a technique very similar to the one given by Phillips (1974). Phillips technique was modeled after Arakawa's (1972) energy conserving vertical integration technique. We will only summarize the basic technique here. Phillips (1974) and Brown (1974) gave a more detailed description. First we define

$$\hat{\sigma}_k = 1 - \sum_{\ell=1}^{k-1} \Delta_\ell \quad ; \qquad \sum_{\ell=1}^{k} \Delta_\ell = 1 \tag{12.34}$$

where Δ_ℓ is the separation between sigma levels k and k+1, see Fig. (12.1). Next define

$$\sigma = \frac{p - p_T}{p_\sigma} \tag{12.35}$$

$$\hat{\sigma}_k = \frac{\hat{p}_k - p_T}{p_\sigma} \tag{12.36}$$

where the hat ($\hat{}$) denotes a variable at the whole level, while the absence of the ($\hat{}$) represents a variable at the intermediate levels and p_T is pressure at the top of a given sigma domain. Now the geopotential can be computed as follows:

a. Forecast p_σ from (12.12) then determine

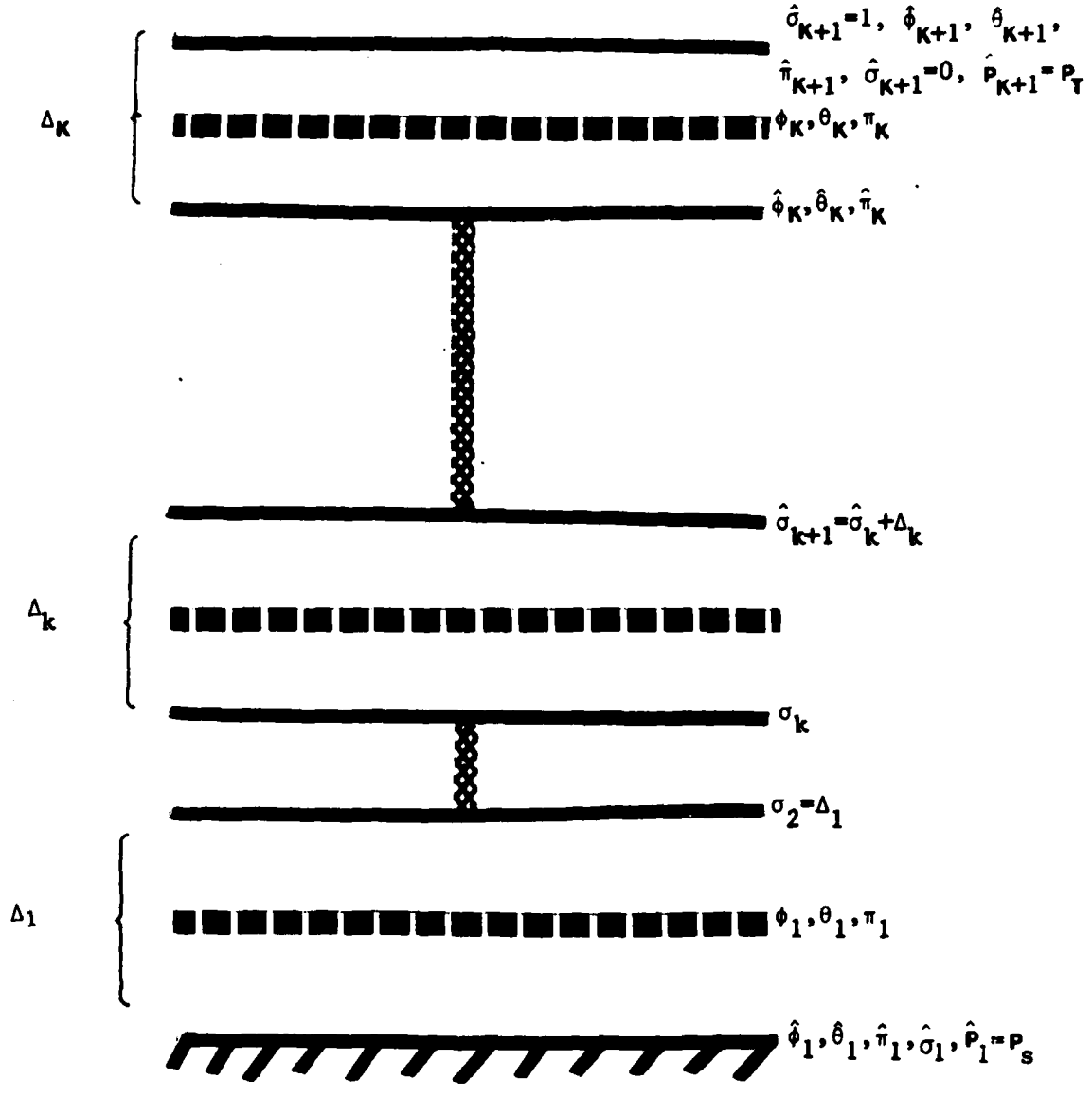

Figure 12.1. Generalized depiction of variable location for computing the geopotential height using the method given by Phillips (1974).

$$\hat{p}_k = p_T + p_\sigma \hat{\sigma}_k \quad . \tag{12.37}$$

b. Compute Exner's function for the whole levels.

$$\hat{\pi}_k = \left(\frac{\hat{p}_k}{p_0}\right)^\kappa ; \quad \kappa = R/C_p \tag{12.38}$$

c. Compute π_k from

$$\pi_k = \frac{1}{p_0^k} \frac{\hat{p}_k^{1+\kappa} - \hat{p}_{k+1}^{1+\kappa}}{(1+\kappa)(\hat{p}_k - \hat{p}_{k+1})} \quad . \tag{12.39}$$

d. Compute predicted values of $\hat{\theta}_k$ from the predicted values of θ_k and θ_{k+1}.

$$\hat{\theta}_k = \tfrac{1}{2}(\theta_k + \theta_{k+1}) \quad . \tag{12.40}$$

This formulation conserves θ^2 .

e. Determine ϕ_1 from

$$\phi_1 = \hat{\phi}_1 + C_p \left\{ \sum_{k=1}^{k-1} \hat{\sigma}_{k+1} \left\{ (\phi_k - \phi_{k+1}) \left[\tfrac{1}{2}(\pi_k + \pi_{k+1}) - \hat{\pi}_{k+1} \right] \right\} + \phi_1 (\hat{\pi}_1 - \pi_1) \right\} \tag{12.41}$$

where $\hat{\phi}_1$ is the surface value of the geopotential.

f. Finally, determine the geopotential, ϕ_k , k=2,3,...,K from

$$\phi_{k+1} - \phi_k = C_p(\pi_k - \pi_{k+1})\hat{\theta}_k \quad . \tag{12.42}$$

The above technique is used in 7L AWSPE routine GEOPTL which was adapted from NMC's 7L PE routine GEOP7L.

12.10 Dry Convective Adjustment.

The 7L AWSPE model applies a dry convective adjustment procedure to maintain model stability. If this procedure is not used, the phase speed of internal gravity waves becomes unstable (complex) when superadiabitic conditions exist.

The procedure used to apply the dry convective adjustment was taken directly from the NMC 7L PE model software. A similar procedure is outlined in Haltiner and Williams (1980) and will be repeated here. Both of the schemes conserve total potential energy; that is,

$$\int_{z_3}^{z_T} C_p \delta T \rho dz = \frac{C_p}{g} \int_{p_T}^{p_B} \delta T dp = 0 \tag{12.43}$$

where T and B represent the top and bottom of the unstable layer, respectively. Physically, dry convection develops whenever the lapse rate exceeds the dry adiabatic value. This transports heat upward until a neutral lapse rate results. Thus, potential energy is converted to kinetic energy which is eventually converted into heat. The result is a total energy redistribution of potential temperature.

The 7L AWSPE essentially uses a formulation similar to (12.43) to solve for the energy conserving readjustment of temperature. For one unstable layer between levels k and k+1, (12.43) can be written as

$$(T + \delta T_k)\left(\frac{1000}{p_k}\right)^{R/C_p} = (T_{k+1} + \delta T_{k+1})\left(\frac{1000}{p_{k+1}}\right)^{R/C_p} \tag{12.44}$$

where

$$\delta T_k = -\delta T_{k+1} \quad . \tag{12.45}$$

Thus (12.44) and (12.45) can be solved for δT_k and δT_{k+1} to get the dry convective adjustment to the temperature field. A very similar technique is applied at all levels in the 7L AWSPE model to ensure no superadiabatic lapse rates are allowed to exist.

12.11 Fourth-Order Versus Second-Order Differencing.

The 7L AWSPE can use either fourth-order or second-order finite differencing for the advection terms in the equations of motion. Campana (1978) found that fourth-order differencing greatly improved forecast accuracy. Table 12.1 presents his results and demonstrates the expected improvement in the fourth-order version of the 7L AWSPE as compared to the second-order version.

Table 12.1 contains the 500-mb RMS vector wind error and 500-mb mean RMS temperature error at 48h. Note that the fourth-order 1-bedient 7L PE verifies almost as well as the (then operational) second-order half-bedient NMC 7L PE. The improved forecast accuracy of the fourth-order NMC 7L PE (a moist version of the 7L AWSPE) is impressive when compared to the NMC 6L PE (a moist version of the 6L AWSPE).

Haltiner and Williams (1980) showed fourth-order differencing improves phase speed accuracy for waves whose length is 4 to 12 grid increments (DX) for the simple advection equation. Here DX refers to the separation between adjacent grid points in the model (1-bedient for the 6L and 7L AWSPE models). Thus, the improved forecast accuracy found in Campana's (1978) fourth-order results was due to improved forecasts of phase speeds for wavelengths of four grid increments and larger.

Table 12.1. Fourth-order versus second-order finite differencing forecast accuracies for selected cases (Campana, 1978)

MEAN 500-mb (48-h) RMS Vector Wind Error (m s^{-1})	NMC 6L PE (1-bedient)	OPNL Second Order NMC 7L PE (1/2-bedient)	Fourth Order NMC 7L PE (1-bedient)
1000 mb	9.53	7.67	7.82
500 mb	11.13	8.66	8.89
300 mb	16.26	12.77	13.04
100 mb	--	8.13	8.27
Mean (48-h) RMS 500-mb Temperature Error (^{o}C)			
1000mb	3.78	3.13	3.16
500mb	3.06	2.51	2.56
300mb	3.08	2.57	2.59
100mb	--	3.48	3.53

*Cases were: 9 Jan 75 12Z, 11 Jan 75 00Z, 21 Feb 75 00Z, 5 Dec 76 12Z, 1 Jul 77 00Z.

13. THE 7-LAYER AWSPE MODEL MARCHING PROCESS.

The finite-difference equations for the second-order model are solved in the following manner. For the fourth-order model replace (12.9) through (12.12) with (12.13) through (12.16). Given initial values for u, v, θ, and p_σ, future values of these variables are computed using (12.9) through (12.12). To apply pressure-gradient averaging, the future values of p_σ and θ must be computed before the pressure-gradient force can be calculated. Thus, $\dot{\sigma}$ is computed using the method given in Section 12.3. Then p_σ is forecast from (12.12), and θ is computed using (12.11). The pressure at all levels is computed for the future time step N+1 (where N represents an arbitrary time step) by summing p_σ downward from the top level (0), where p = 50 mb. Now Exner's function, π , at N+1 is computed from

$$\pi = \left(\frac{p}{p_0}\right)^{R/C_p} \tag{13.1}$$

where p_o = 1000 mb. The technique given in Section 12.9 is then used to compute the heights, z, at the intermediate levels for time N+1 given the terrain height at level 7. Finally, the pressure-gradient force can be computed from the values of z and π at times (N-1, N, N+1) using (3.12). Then (12.9) and (12.10) are solved for the values of u and v at time step N+1. We repeat this process in time until the desired forecast length is reached. After the first time step, a centered finite difference scheme is used for the time derivative. Because pressure-gradient averaging is used in the model, a time step of 1200s is permitted for the second-order version. For the fourth-order version the time step must be reduced to 900s. For the first time step, both models use a forward-finite-difference scheme. A forward scheme is also used for surface drag and sea surface heating terms.

14. INITIALIZATION.

The initialization process is detailed in Shuman and Hovermale (1968). This process for the 7L AWSPE is identical to that given in Section 5, Part I, with two exceptions. First, data from the AFGWC High Analysis Model (HIANAL) at 50 mb are used to compute values for the top layer of the model. Values in the top layer of 6L AWSPE model are chosen in a more arbitrary manner. Second, the nonlinear balance equation is used vice the linear balance equation in Part I.

15. OUTPUT FIELDS.

The 7L AWSPE model produces the same pressure-coordinate data base as the 6L AWSPE (Section 6). The technique used to convert 7L AWSPE sigma-coordinate forecast fields to the pressure-coordinate data base is also identical to that used by the 6L AWSPE (Section 6).

16. A DESCRIPTION OF THE SUBROUTINES AND MAJOR ARRAYS USED IN THE 7-LAYER AWSPE PROGRAM.

In this section we describe the subroutines used in the 7-Layer AWSPE program. Then we present a description of the major common blocks and arrays used throughout the model. This section is intended for those requiring a more detailed knowledge of the 7L AWSPE. Further explanation of the actual details of the model can be found in the in-line program documentation. Figs. 16.1, 16.2, and 16.3 give the 7L AWSPE model subroutine flow diagram. The numbers represent the order in which the individual routines are called. The basic functions of each subroutine are given below.

PEFCST- The main routine or driver for the 7L AWSPE model. It sets constants, reads @SETC information, inputs the initial data on sigma coordinates from absolute PEINIT, produces the desired forecast, and outputs the forecasts to files for conversion to the pressure-coordinate data base.

BALNCE- Computes the u and v components of the wind from the sigma surface geopotential using the nonlinear balance equation.

BALUV- Computes the wind from the height and Exner's function on a sigma surface using the nonlinear balance equation.

BNDRY- Computes the u and v boundary conditions by applying the "diffusive nudge" boundary conditions. (Section 12.4).

BTDRY- Computes the θ and p_σ boundary conditions by applying the "diffusive nudge" boundary conditions. (Section 12.4.)

BNDSET- Computes the Laplacian of the the initial boundary values (6 grid rows). These values are used by subroutine BNDRY to compute the "diffusive nudge" lateral boundary conditions. (Section 12.4).

DIAG - Computes all diagnostic energetics.

DIV- Computes the divergence on the earth. This diagnostic information is not used by the 6L AWSPE model.

DRY- Applies dry convective adjustment to the forecast potential temperature field. If θ above is less than θ below, then the scheme adjusts the two potential temperatures to produce a neutral lapse rate. (See Section 12.10)

FCST- Forecast module driver. This routine forecasts future values of u, θ, v, and p_σ using centered time differencing with a time step of 2 *DT seconds (where DT=1200 s for second order and DT = 900 s for fourth order). Forecast is computed on a polar stereographic projection.

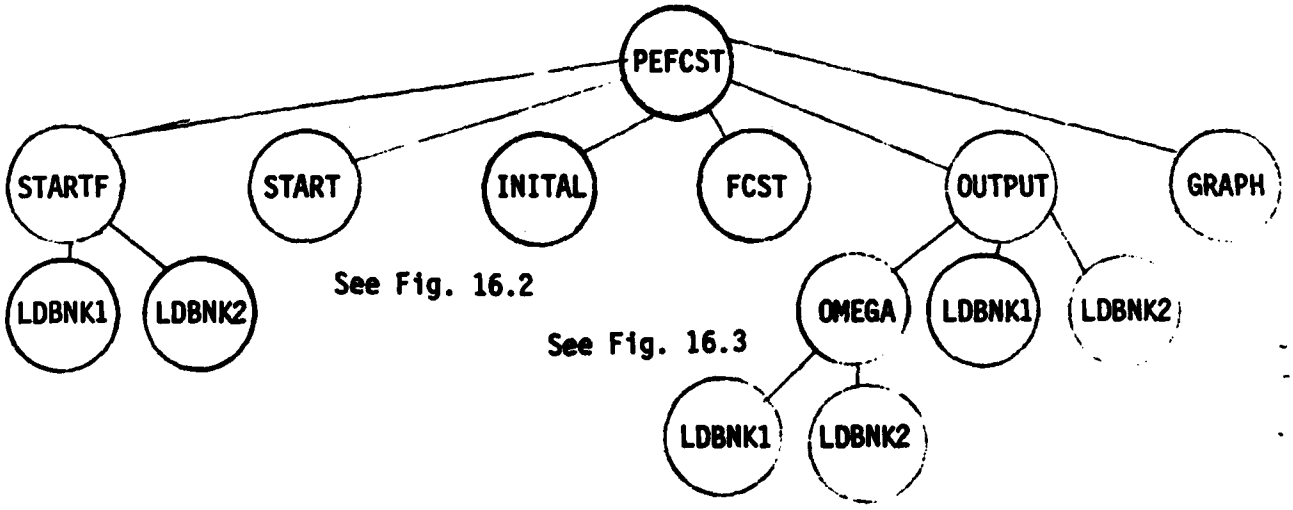

Figure 16.1. The subroutine flow diagram for the Lower Portion of the 7L AWSPE Model.

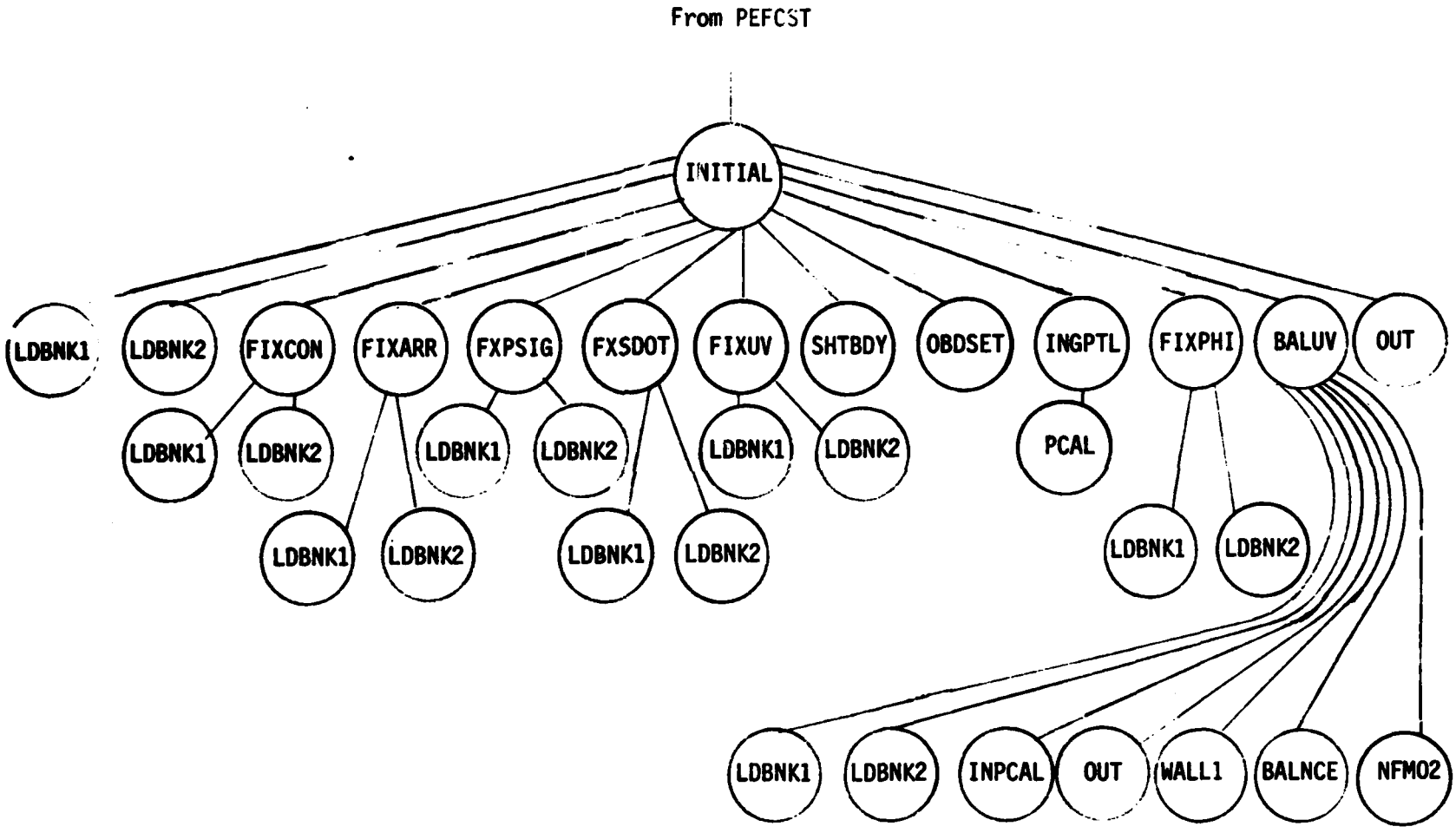

Figure 16.2. The Subroutine Flow Diagram for the Initializer Portion of the 7L AWSPE Model.

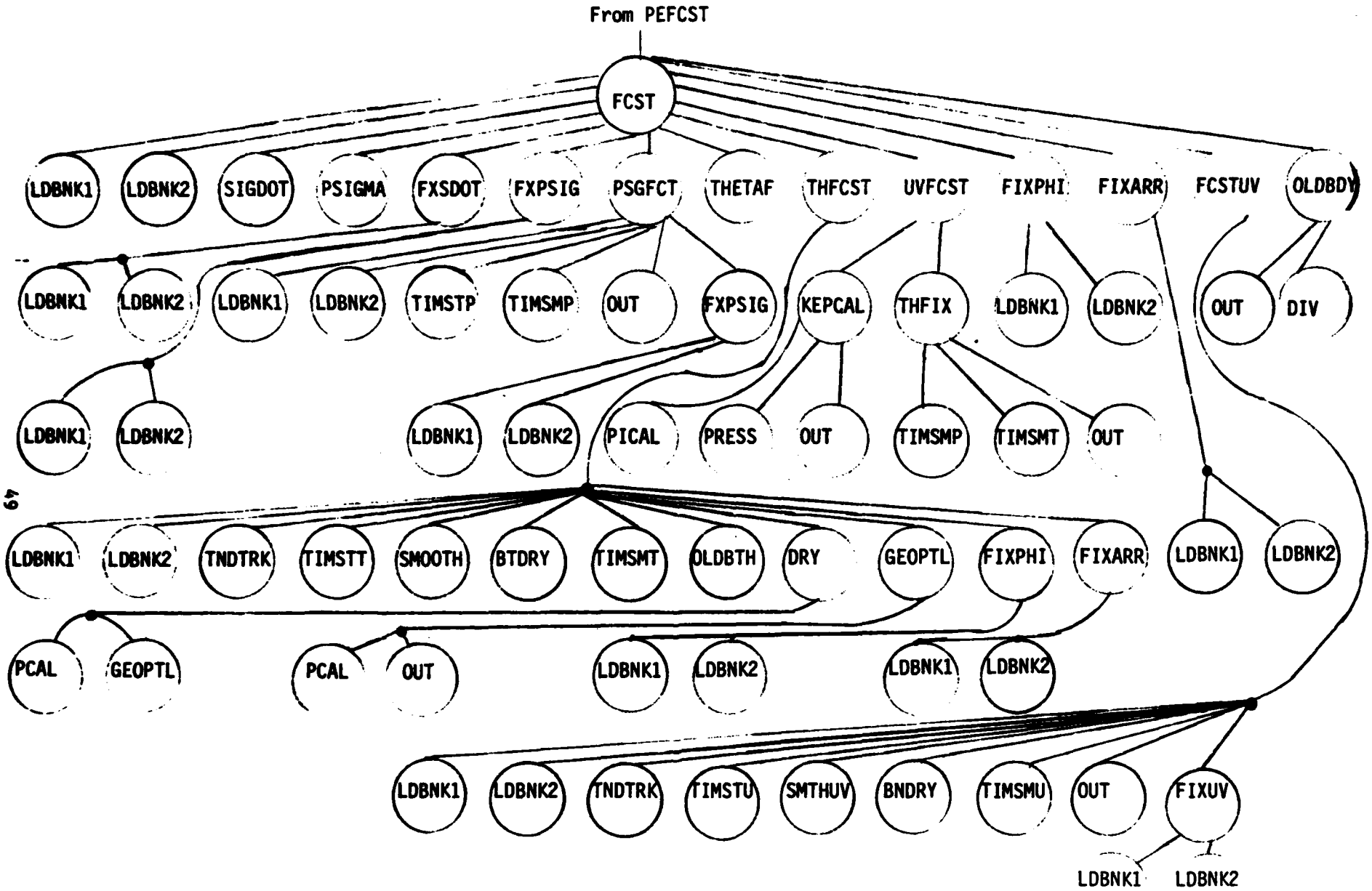

Figure 16.3. The subroutine flow diagram for the forecaster portion of the 7LAWSPE Model.

FCSTUV- Given the tendency values computed by UVFCST, it forecasts u and v at the next time step. It then adjusts the boundary values and applies space and time smoothing.

FILERR- This is an I/O error termination routine.

FIXARR- Switches the overlap areas of each Data-Bank for the potential temperature array (THETA). That is, it stores rows 27 and 28 from D-Bank 1 into rows 31 and 32 in D-Bank 2. It then store rows 33 and 34 from D-Bank 2 into rows 29 and 30 in D-Bank 1.

FIXCON- Switches the overlap areas of each D-Bank for the land-sea indicator, the sea surface temperature, the drag coefficient, the map factor, and the Coriolis parameter. Same as FIXARR for the sea surface temperatures, the drag coefficient, the map factor, and the Coriolis parameters.

FIXPHI- Same as FIXARR only for the geopotential height field.

FIXWRK- Transfers values from the left side (J=33, 34) of that portion of the work array where J=31, 61 to the right side (J=29, 30) of the work array where J=1, 30. Values are then transferred from the right side (J=27,28) of that portion of that work array where J=1,30 to the left side (J=31, 32) of that portion of the work array where J=30,61.

FIXUV- Switches the overlap areas of each Data-Bank for the u and v wind component arrays. It stores rows 27 and 29 from D-Bank 1 into rows 31 and 32 in D-Bank 2. It then stores rows 33 and 34 from D-Bank 2 into rows 29 and 30 in D-Bank 1.

FXPSIG- Same as FIXARR, except for the p_σ array.

FXSDOT- Same as FIXARR, except for the $\dot{\sigma}$ array.

GEOPTL- Computes the geopotential height field at all levels for a given time. The method used here follows from Brown (1974) and Phillips (1974), see Part II, Section 12.9. This method was first developed by Arakawa and an example of the procedure is given in Arakawa (1977). The code used here follows directly from NMC's subroutine GEOP7L.

GEOPTL1- Same as GEOPTL except it computes the geopotential height for a single grid point.

GEOPTL2- Computes the geopotential height field at all levels for a given time. (Section 3.9).

GRAPH- Diagnostic program that prepares a graph of the 7L AMSPE model kinetic energy amplification with respect to time. This is a diagnostic routine only.

HEAT- Computes the only diabatic term used by the 7L AWSPE. Sea surface heating is parameterized using the specification given by Shuman and Hovermale (1968). Other diabatic forcing terms could be added here. (Section 12.5).

INITIAL- Reads the initial data file produced by absolute PEINIT. For a normal @XQT the initial data is stored on file 10. Otherwise files L3HR and 99 are used as the current and current minus one time steps in order to start with leapfrog time differencing. The initial fields are on the sigma coordinate system shown in subroutine FCST. The routine does the following: First, it determines whether this is a restart or a forecast starting from time 0. Next, the data are retrieved and stored in the proper arrays. The subroutine calls GEOPTL to compute the height field in preparation for the first time step. Finally, diagnostic output fields are generated, if requested.

INITL2- Initializes the model with Rossby-Haurwitz waves to test the model numerics. Many other initializations are available in this test routine. This is only a test routine.

KEPCAL- Computes the product of the kinetic energy and the map factor for use in UVFCST. Place the result in E (I, 1, 1, k). Computes the pressure gradient force for UVFCST.

LDBNK1- Sets the D-Bank pointer or Bank Descriptor Index (BDI) to D-Bank 1. The arrays in common blocks FIELD1 and FIELD2 are mirror images of one another. Common block FIELD1 contains all arrays that are mapped into D-Bank 1 and common block FIELD2 contains all arrays that are mapped into D-Bank 2. The array names in FIELD2 are treated as dummy names and are never referenced by the model, but the storage locations are used by changing the Bank Descriptor Indicies (BDI) through calls to LDBNK1 and LDBNK2.

LDBNK2- Same as LDBNK1 except it sets the BDI or D-Bank pointer to D-Bank 2.

NFM02- Smooths the wind field after it is nonlinearly balanced to the height field.

OBDSET- Applies the old 6L AWSPE model lateral boundary conditions to θ and p_σ (Section 3.4). This routine is used during the initialization process.

OLBDTH- Same as OBDSET except this routine is used during the 7L AWSPE model marching process.

OLDBRY- Applies the old 6L AWSPE model lateral boundary conditions. These conditions are applied to u and v in this routine. (Section 3.4).

OMEGA- Computes OMEGA for use by applications programs and AFGWC/WF forecasters. This is a diagnostic routine only. See section 12.8.

OUT- Displays a 53 X 57 array. One half of the array will be displayed per page. If less than 7 levels are requested, the routine outputs starting from the bottom level.

OUTPUT- Checks to see if it is time to store into the data base files. Every three hours, data will be stored in the files. Every 12 hours, either PE12, PE24, PE36, or PE48 will be started to store the data into the pressure-coordinate data base.

PICAL- Computes Exner's function at the intermediate vertical levels using (12.37). This technique helps to conserve energy in the calculation of the pressure gradient force.

PRES- Computes the pressure of each point on the sigma surface.

PSGFCT- Forecasts p_σ at the next time step from the tendency value which is computed by PSIGMA. The boundary values are adjusted and the forecast values are time smoothed.

PSIGMA- Computes the tendency of p_σ for the model troposphere and stratosphere. p_σ is a constant (50mb) in the (one-layer) boundary layer. To compute p_σ , we use (12.12) or (12.16) from Section 12.1.

SHTBDY- Applies the old 6L AWSPE model boundary conditions. Here, these conditions are only applied to the terrain heights to prevent noise on the boundaries caused by variable terrain at the boundary. See Section 3.4.

SIGDOT- Computes the sigma coordinate vertical motion, $\dot{\sigma}$ at time "N" for use in the tendency equations. (Section 12.3.)

SMOOTH- Smooths array ANM1 (time level N -1) and then adds the result to array ANP1 (time level N+1). Space smooths the θ and p_σ fields. (Section 12.6).

SMTHUV- Same as SMOOTH except for u and v.

START- This routine is called by main program PEFCST to retrieve the @SETC information. The many @SETC options available are given in Table 16.1.

STARTF- Sets the basic parameters for the 7L AWSPE model, e.g., time step, gas constants, gravity, etc.

THETAF- Computes potential temperature tendency from (12.11) or (12.15).

THFCST- Computes the potential temperature at the next time step given the tendency from THETAF. The forecast values are space smoothed.

TABLE 16.1 Start Options for the 7L AWSPE Model.

DOCUMENTATION OF SETC WORD			
FUNCTION "BITS" BIT (1-36)	SETC BIT (0-35)	NUM	STATE
13	12	1	Use 47*51 Fields to Initialize
13	12	0	Use 53*57 Fields to Initialize
13	13	1	Contingency 72 to 96HR Forecast
14	13	0	No 72 to 96HR Contingency Forecast
15	14	1	Diagnostic Print
15	14	0	No Diagnostic Print
16	15	1	Extended 48-72HR PE Forecast
16	15	0	Non Extended 48-72HR Forecast
17	16	1	Off-time PE (06 and 18Z)
17	16	0	On-time PE (00 and 12Z)
18	17	1	Update (00-06)
18	17	0	No update
19,20,21,18,19,20	3-BITS		These Bits Are Used to Compute the Forecast Start Hour
22	21	1	No Internal Start of PE12, PE24...
22	21	0	Do Internal Start of PE12, PE24,...
23,24	22,23	0	MAXTIM = 48
23,24	22,23	1	MAXTIM = 12
23,24	22,23	2	MAXTIM = 24
23,24	22,23	3	MAXTIM = 36

These bits determine the forecast finish hour

THFIX- Time smooths the potential temperature and geopotential height. Moves the potential temperature (THETA array) and geopotential height (PHI array) forecasts into the current (N) time step. Moves potential temperature and geopotential height from the current time step into the last time step. This routine is called by UVFCST to allow u and v at the future time step to be stored in the arrays THETA and PHI after the pressure-gradient force is computed.

TIMSMP- Time smooths the P-Sigma array valid at time N to avoid time splitting. The array valid at time N is then used as the starting point for the next time step; that is, the N array becomes the N-1 array for the next time step.

TIMSMT- Same as TIMSMP except time smoothes the potential temperature.

TIMSMU- Same as TIMSMP for the u and v wind components.

TIMSTP- Uses a centered time step to compute the N+1 time step of p_σ given the tendency value and value at the N-1 time step.

TIMSTT- Same as TIMSTP for potential temperature.

TIMSTU- Same as TIMSTP for the u and v wind components.

TNDTRK- Truncates the tendencies of u, v and potential temperature below 20 degrees north.

UVFCST- Computes the tendencies of u and v (12.9) and (12.10) or (12.13) and (12.14). (Section 12.2)

We present the description of the major arrays used throughout the 7L AWSPE model in Table 16.2.

Table 16.2. List of Major Arrays Used by the 7L AWSPE Model.

Common Blocks FIELD1/FIELD2

The arrays in common blocks FIELD1 and FIELD2 are mirror images of one another. Common block FIELD1 contains all arrays that are mapped into D-BANK1 and common block FIELD2 contains all arrays that are mapped into D-BANK2. The array names in FIELD2 are treated as dummy names and are never referenced in the model equations, but the storage locations are used by changing the bank descriptor index (BDI).

ARRAY NAME		DESCRIPTION
CD (53, 1, 1, 31)	-	CD (I, 1, 1, J) surface drag coefficient.
F (53, 1, 1, 31)	-	F (I, 1, 1, J) Coriolis parameter.
IMAX (31)	-	Maximum I index for half grid points, function of 31 J Values.
IMAXW (31)	-	Maximum I index of whole grid points, function of 31 J values.
IMINW (31)	-	Minimum I index for whole grid points, function of 31 J values.
JMAX	-	Maximum J index for half grid points.
JMAXM1	-	JMAX-1
JMAXM2	-	JMAX-2
JMAXW	-	Maximum J index for whole grid points.
JMIN	-	Minimum J index for half grid points.
JMIN(31)	-	Minimum I index for half grid points, function of 31 J values.
JMINW	-	Minimum J index for whole grid points.
JMINP1	-	JMIM+1
JMINP2	-	JMIN+2
JMNWP1	-	JMINW+1
JMNWP2	-	JMINW+2
JMXWM1	-	JMAXW-1
JMXWM2	-	JMAXW-2
PHI (53, 7, 3, 31)	-	PHI (I, K, T, J), hgt field For 7 vertical levels and 3 time levels. Also used to hold N+1 time levels of u for u forecast.
PI (53, 1, 3, 31)	-	PI (I, 1, T, J), Exner's function for three time levels and one vertical level.
PIVAL (3000)	-	PIVAL (2*PRESSURE (MB)) - Value of PI every 0.5 mb from 5 to 1500mb
PSIG (53, 2, 3, 31)	-	PSIG (I, KK, T, J), p-sub-sigma for troposphere and stratosphere and three time levels.
RLNDSE (53, 1, 1, 31)	-	RLNDSE (I, 1, 1, J), sea level indcator (0 for sea, 0.0001 for land)
RM (53, 1, 1, 31)	-	RM (I, 1, 1, J), map factor squared with xy overbar applied (half grid point values)
RMAP (53, 1, 1, 31)	-	RMAP (I, 1, 1, J), map factor squared at the whole grid points.

SDOT (53, 6, 1, 31)	-	SDOT (I, K-1, I, J) sigma dot for levels 2 - 7, levels 1 and 8 are zero.
SHGT (53, 1, 1, 31)	-	SHGT (I, 1, 1, J), terrain height times acceleration of gravity.
THETA (53, 7, 3, 31)	-	THETA (I, K, T, J), potential temperature for 7 vertical levels and 3 time levels. Also used to hold N+1 time level of v for in UVFCST.
TSEA (53, 1, 1, 31)	-	TSEA (I, 1, 1, J), sea surface temperature (K) (climatological values).
U (53, 7, 2, 31)	-	U (I, K, T, J), u time levels N-1 and N.
P (53, 1, 1, 31)	-	UP (I, 1, 1, J), work array for the u forecast.
V (53, 7, 2, 31)	-	V (I, K, T, J), v at time levels N-1.
VP (53, 1, 1, 31)	-	VP (I, 1, 1, J), work array for the v forecast.

COMMON BLOCK FIELD

ARRAY NAME		DESCRIPTION
WORK (53, 4, 1, 61)	-	WORK (I, IW, 1, J+JJ), where IW is the work area, JJ=(IHALF-1)*30, J=1, 31, and IHALF=2 for dual bank. version. WORK is a work array used throughout the model.
WORK2 (53, 2, 1, 61)	-	WORK2 (I, IW, 1, J+JJ), additional work area.

COMMON BLOCK HALF

ARRAY NAME		DESCRIPTION
IHALF	-	DBANK INDICATOR (1 or 2)

COMMON BLOCK PAR

ARRAY NAME		DESCRIPTION
BTHICK	-	Thickness of the boundary layer (50 mb).
CP	-	Specific heat at constant pressure (CP=1004.67).
CTDX	-	Delta T/Delta X = 2400 s/381000 m.
DX	-	Delta X=381000,M.
G	-	Acceleration of gravity. G=9.81 m/s.
RKAPA	-	Constant used in GEOPTL (1./(1.+ROCP))*(1000)***ROCP.
R	-	Ideal gas constant (R=287.04)
RDLX	-	1/DX=1./381000(1/m).
RDLY	-	1/DY=1./381000(1/m).
RDT	-	1/DT=1.2400(1/s).
ROCP	-	R/CP.

COMMON BLOCK IBARO

ARRAY NAME		DESCRIPTION
IBAR	-	If one, run barotropic version. If zero, run baroclinic version.

COMMON BLOCK FIXER

ARRAY NAME		DESCRIPTION
KTMAX	-	Maximum number of vertical layers.
KTPMAX	-	KTMAX+1, maximum number of vertical levels.
KPMAX	-	Maximum number of P-sigma layers.
IHMAX	-	Maximum number of data banks (the maximum allowable number is 2).

COMMON BLOCK TUNER

ARRAY NAME		DESCRIPTION
AFACL6	-	Pressure-gradient-averaging factor for less than 6 hours.
AFACG6	-	Pressure-gradient-averaging factor for more than 6 hours.
RMU1	-	Smoothing coefficient for latitudes less than 20N.
TSMTH	-	Time smoothing coefficient.

17. SUMMARY.

In Part II, we have discussed the numerical, mathematical, and high level program design of the 7L AWSPE model. The 7L AWSPE is a dry version of the NMC 7L PE described by Campana (1978).

We developed the 7L AWSPE for two reasons. First, operational requirements dictated moving the 6L AWSPE from System V to System I. But, the 6L AWSPE could not meet operational timelines when running on System I because of the many I/O operations required by the model. Second, NMC had greatly improved the original Shuman-Hovermale model. Campana's work made it possible for AFGWC to run a fourth-order version of the 7L AWSPE that could produce forecasts almost as well as the 1/2-bedient NMC 7L PE at a fraction of the cost.

Like Campana's (1978) version of the NMC 7L PE, the 7L AWSPE uses the hydrostatic, sigma-coordinate, energy-vorticity form of the primitive equations on a polar stereographic projection of the earth. Two finite-difference formulations of the model exist; a second-order and a fourth-order version. The model domain is identical to the 6L AWSPE and consists of a rectangular area centered at the North Pole. At the outer boundary, a no-slip boundary condition or an isothermal, "nudge" boundary condition can be applied. Terrain is included in the model through the sigma coordinate system. Time and space smoothing are used control temporal and space noise. The only thermodynamic forcing is the parameterization of heat flux from the ocean surface and this is only applied at the lowest layer. Surface drag is parameterized and also applied to the lowest layer only. Pressure-gradient averaging is used to allow a longer time step.

The 7L AWSPE model initialization procedure uses the nonlinear balance equation while the linear balance equation is used by the 6L AWSPE. The 7L AWSPE model forecasts using a centered-time-differencing scheme. The output fields are identical to the 6L AWSPE model.

The 7L AWSPE represents a transfer of technology from NMC to AFGWC. When implemented, the fourth-order version of the 7L AWSPE model will produce significantly improved forecasts of height, temperature, and wind (compared to the second-order 6L AWSPE). The second-order version of the 7L AWSPE should perform only slightly better than the 6L AWSPE. Finally, we note that the 7L AWSPE is a top-down structured, well documented, easily maintainable program, whereas the 6L AWSPE is none of these.

18. REFERENCES

Arakawa, A., 1972: Design of the UCLA general circulation model. Tech Report No. 7, Dept of Meteorology, UCLA.

Brown, J.A., Jr., 1974: On vertical differencing in the sigma coordinate system. NMC Office Note 92, 13 pp.

Brown, J.A., Jr., and K. A. Campana, 1978: An economical time-differencing system for numerical weather prediction. Mon. Wea. Rev., 106, 1125-1136.

Campana, K.A., 1977: Real data experimentation with higher order finite differencing in the semi-implicit version of the Shuman-Hovermale model. NMC Office Note 163, 9 pp.

Campana, K.A., 1978: Real data experiment with a fourth order version of the operational seven-layer model. NMC Office Note 188, 11 pp.

Campana, K.A., 1979a: Higher order finite-differencing experiments with a semi-implicit model at the National Meteorological Center, Mon, Wea, Rev., 107, 363-376.

Campana, K.A., 1979b: 7LPE 4th order coarse mesh backup model. NWS Technical Procedures Bulletin No. 272, 7 pp.

Charney, J.G., 1962: Integration of the primitive and balance equations. Proc. Intern. Symp. Numerical Weather Prediction, Tokyo, Meteorological Society of Japan, 131-152.

Cressman, G.P., 1960: Improved terrain effects in barotropic forecasts. Mon. Wea. Rev., 88, 327-342.

Cressman, G.P., 1963: A three-level model suitable for daily numerical forecasting. Tech Memo No. 22, National Meteorological Center, Weather Bureau, ESSA, US Dept of Commerce, 22 pp.

Flattery, T.W., 1975: The Air Weather Service primitive equation model. AFGWC User Documentation, AFGWC, Air Weather Service (MAC), 12 pp.

Haltimer, G.J., and R.T. Williams, 1980: Numerical Prediction and Dynamic Meteorology. John Wiley and Sons, Inc., New York, NY.

Hoke, J. E., J.L. Hayes, and L.G. Renninger, 1981: Map projections and grid systems for meteorological applications at the Air Force Global Weather Central. AFGWC Tech Note 79/003, AFGWC, Air Weather Service (MAC), 86 pp.

Johnson, A.J., 1975: Air Weather Service primitive equation model program documentation. AFGWC, Air Weather Service (MAC), Offutt AFB, NE, (unpublished manuscript).

Leary, C., 1971: Systematic errors in operational National Meteorological Center primitive-equation surface prognoses. Mon. Wea. Rev., 99, 409-413.

Lorenz, E.N., 1962: Simplified dynamic equations applied to the rotating-basin experiments. J. Atmos. Sci., 19, 39-51.

Palucci, K.J., 1970: AFGWC macro-scale baroclinic prediction model. AFGWC Tech Memo 70-4, AFGWC, Air Weather Service (MAC), Offutt AFB, NE, 11 pp.

Phillips, N.A., 1957: A coordinate system having some special advantage for numerical forecasting. J. Appl. Meteor., 14, 184-185.

Phillips, N.A., 1974: Application of Arkawa's energy-conserving layer model to operational numerical weather prediction. NMC Office Note 104, 39 pp.

Rossby, C.-G., and collaborators, 1939: Relation between variations in the intensity of the zonal circulation of the atmosphere and the displacements of the semi-permanent centers of action. J. Marine Res., 2, 38-55.

Reed, R.J., 1963: Experiments in 1000-mb prognosis. NMC, Weather Bureau, ESSA, Tech Memo 26, U.S. Dept of Commerce, 25 pp.

Shuman, F.G., and J.B. Hovermale, 1968: An operational six-layer primitive equation model. J. Appl. Meteor., 7 , 525-547.

Shuman, F.G., and J.D. Stockpole, 1968: The currently operational NMC model and results of a recent simple numerical experiment. Presented at the WMO/IVGG Symposium on Numerical Weather Prediction, November 26-December 4, 1968, Tokyo, Japan, 10+ pages.

Shuman, F.G., 1977: Some remarks on the use of smoothing and linear diffusion terms to control noise. NMC Office Note 162, 6 pp.

Tarbell, T.C., and J.E. Hoke, 1979: The AFGWC automated analysis/forecast model system. AFGWC Tech Note 79/004, AFGWC, Air Weather Service (MAC), 52 pp.

Teweles, S., and H. Wobus, 1954: Verification of prognostic charts. Bull. Amer. Meteor. Soc., 35, 455-463.

END

FILMED

8-83

DTIC